의학박사 학위논문

Integrated analysis of microbiome and in-depth proteome in chronic rhinosinusitis with nasal polyps

비용종을 동반한 만성 비부비동염에서 미생물과 심층 단백체의 통합 분석

2023년 8월

서울대학교 대학원

의과학과 의과학전공

김 이 숙

A thesis of the Degree of Doctor of Philosophy

Integrated analysis of microbiome and in-depth proteome in chronic rhinosinusitis with nasal polyps

비용종을 동반한 만성 비부비동염에서 미생물과 심층 단백체의 통합 분석

August 2023

The Department of Biomedical Sciences,

Seoul National University

College of Medicine

Yi-Sook Kim

Integrated analysis of microbiome and in-depth proteome in chronic rhinosinusitis with nasal polyps

지도 교수 신 현 우

이 논문을 의학박사 학위논문으로 제출함
2023년 4월

서울대학교 대학원
의과학과 의과학전공
김 이 숙

김이숙의 박사 학위논문을 인준함
2023년 7월

위 원 장 _____ (인)
부위원장 _____ (인)
위 원 _____ (인)
위 원 _____ (인)
위 원 _____ (인)

Integrated analysis of microbiome and in-depth proteome in chronic rhinosinusitis with nasal polyps

by

Yi-Sook Kim

A thesis submitted to the Department of Biomedical Sciences in partial fulfillment of the requirements for the Degree of Doctor of Philosophy in Biomedical Sciences at Seoul National University College of Medicine

April 2023

Approved by Thesis Committee:
July 2023

Chair _____(Seal)

Vice Chair _____(Seal)

Examiner _____(Seal)

Examiner _____(Seal)

Examiner _____(Seal)

ABSTRACT

Integrated analysis of microbiome and in-depth proteome in chronic rhinosinusitis with nasal polyps

Yi-Sook Kim
The Department of Biomedical Sciences
The Graduate School
Seoul National University

Chronic rhinosinusitis (CRS) is defined as inflammation of the nasal and paranasal sinus mucosa and exhibits remarkable heterogeneity. Although antibiotics are prescribed frequently to reduce inflammation, effects of antibiotics on nasal environment and host response in CRS is clearly unknown. Therefore, I aimed to reveal the associations between nasal environment and host response using integrated analysis. For in-depth investigation, filter papers were used to obtain nasal secretions from middle meatus. The nasal secretions were collected from 29 controls, 30 patients with CRS without nasal polyp (CRSsNP), and 40 patients with CRS with nasal polyp (CRSwNP). To identify the effects of antibiotics, 99 subjects were divided on whether they had taken antibiotics 3 months prior to sampling. Then, metagenomic sequencing and mass spectrometry-based proteomic analysis were performed. I revealed the associations between the microbiome and secreted proteome could be altered in relation to the use of antibiotics. Furthermore, I identified the use of antibiotics might have stronger effects on not only nasal microbiome and secreted proteome, but also associations between them in CRSwNP compared to those in control and CRSsNP subjects. Although it is not

clear whether the global changes caused by antibiotics are favorable or unfavorable to treat CRS, I suggest that the use of antibiotics need to be regarded as an essential confounding factor in the microbiome and proteome analysis. These findings allow us to obtain new insight on the nasal environment and host response in CRS.

Keywords: Sinusitis; Nasal polyps; Proteomics; Metagenomics; Anti-bacterial agents

Student Number: *2017-26948*

Contents

List of tables and figures

List of abbreviations

ABX: The subjects who had taken antibiotics 3 months before sampling

aSPC: Adaptive sum of powered correlation

CRS: Chronic rhinosinusitis

CRSsNP: Chronic rhinosinusitis without nasal polyp

CRSwNP: Chronic rhinosinusitis with nasal polyp

DDA: Data-dependent acquisition

DEPs: Differentially expressed proteins

DFa : Decreased families in ABX group

DFc : Decreased families in CRSwNP patients

DIA: Data-independent acquisition

DPa : Decreased proteins in ABX group

DPc : Decreased proteins in CRSwNP patients

GO: Gene ontology

IFa : Increased families in ABX group

IFc : Increased families in CRSwNP patients

IPA: Ingenuity pathway analysis

IPa : Increased proteins in ABX group

IPc : Increased proteins in CRSwNP patients

LC-MS: Liquid chromatography-tandem mass spectrometry

LDA: Linear discriminant analysis

LEfSe: Linear discriminant analysis effect size

L-M: Lund-Mackay

MS: Mass spectrometry

NABX: The subjects who had not taken antibiotics 3 months before sampling

NP: Nasal polyp

OTU: Operational taxonomic unit

PCoA: Principal coordinates analysis

PERMANOVA: Permutational multivariate analysis of variance

SPT: Skin prick test

INTRODUCTION

Chronic rhinosinusitis (CRS) is defined as inflammation of the nasal and paranasal sinus mucosa that lasts at least 12 weeks[1] and one of the most frequent upper airway diseases in Western and Asian countries.[2, 3] As this disease exhibits remarkable heterogeneity, researchers have investigated endotypes of CRS. According to the studies, the endotypes were characterized by cytokines[4], symptoms[5], microbiota composition[6], and clinical characteristics.[7]

So far, to identify the endotypes, nasal samples were usually collected by biopsy[4], lavages[8], swabs[9], and scraping[10]. As the nasal samples obtained by non-invasive procedure could sufficiently reflect the current disease state, non-invasive approaches like lavages and swabs are preferred. However, only limited number of proteins have been detected in the nasal samples compared to other samples obtained by non-invasive procedure like urine and saliva.[11] Herein, I sought to suggest a sampling method for collecting nasal secretions using filter papers. The adsorbed nasal proteins was easily bound to the paper and preserved.[12] Furthermore, it could allow us to enhance site-specificity and analyze relatively less diluted samples.[13]

Recently, for better understanding of human diseases, various studies have been conducted from multiple perspectives with multi-source data.[14] For example, in inflammatory bowel disease, host profiles were obtained from both proteomic and metabolomic analyses in serum and microbial profiles identified by metagenomics in stool.[15] It showed that microbiome could regulate concentration of luminal short-chain fatty acid and succinate that might control the course of inflammation. On the other hand, metagenome and metabolome in induced sputum and host proteome

and transcriptome revealed that microbiome-derived metabolites could alleviate inflammation via cell cross-talk mediated by IL-22 in chronic obstructive pulmonary disease.[16] According to the results, profiles of microbiome and molecular changes in the host should be considered together. Thus, to obtain better understanding of CRS, I sought to reveal the associations between nasal environment and host response using metagenomic and proteomic analyses, respectively.

Antibiotics are prescribed frequently to patients with CRS, although there is lack of evidence to support benefits of them.[17, 18] However, the use of antibiotics have not been taken into account in the most of previous studies in CRS patients.[6, 9, 19-33] Thus, it is not clear about the effects of antibiotics on nasal microbiome, epithelium, and associations between them.

Here, I aimed to investigate the associations between microbiome (nasal environment) and secreted proteome (host responses) in relation to disease status using integrative analysis. To conduct in-depth analysis, nasal secretions were collected on the filter papers. Furthermore, I sought to determine the effects of antibiotics on nasal environment, host response, and associations between them. These findings help us to better understand the nasal environment and host response in CRS and how antibiotics, which are used to relieve symptoms of CRS, affect the treatment of CRS.

MATERIALS AND METHODS

Study design and collection of nasal secretions

The study was approved from Internal Review Board of Seoul National University Hospital (No. C-1308-099-515) and all subjects had given written informed consent. Chronic rhinosinusitis (CRS) was defined according to the 2012 European position paper on rhinosinusitis and nasal polyps guidelines.[1] It was diagnosed by history taking, physical examination, nasal endoscopy, and sinus computed tomography. Patients with deviated nasal septum but without sinonasal disease were considered as control group. The exclusion criteria were as follows: less than 14 years of age and patients with unilateral rhinosinusitis, allergic fungal sinusitis, antrochoanal polyps, cystic fibrosis, or immotile ciliary disease. The demographic characteristics were described in Table 1 and 2.

Nasal secretions were acquired from both sides of the nose using sterilized strips of filter papers (7 × 30 mm; Whatman No. 42, Whatman, Clifton, USA) as previously reported.[34, 35] The paper was placed on the middle meatus for 10 minutes. The two papers from each subject were stored into a tube and 1ml of nuclease-free water was added. The tubes were rotated for 1 hour at room temperature. Then, the aqueous samples (nasal secretions) were stored at -70℃ until analysis.

To determine the number of eosinophils and neutrophils, the sinonasal tissue was obtained during endoscopic sinus surgery. After embedded in paraffin, it was cut into 5-mm sections and stained with hematoxylin and eosin (H&E). Eosinophils and neutrophils were counted in 3 high power fields (x400) per section under light microscope.

Table 1. Demographic characteristics of cohort 1 (DDA set) and 2 (DIA set)

Sample	Age (y)	Sex	Asthma	Polyps	Atopy	L-M score	
						Left	Right
Cohort 1							
Control_1	27	M	N	N	N	0	0
Control_2	15	M	N	N	N	0	0
Control_3	52	M	N	N	N	0	0
Control_4	52	M	N	N	N	0	0
Control_5	55	M	N	N	N	0	0
CRSsNP_1	29	M	N	N	N	9	4
CRSsNP_2	39	M	N	N	Y	10	9
CRSsNP_3	25	F	N	N	Y	6	5
CRSsNP_4	44	M	N	N	Y	4	4
CRSsNP_5	57	F	N	N	N	2	9
CRSwNP_1	39	M	N	Y	N	3	12
CRSwNP_2	62	F	N	Y	N	6	8
CRSwNP_3	14	M	N	Y	N	12	10
CRSwNP_4	53	M	N	Y	N	12	12
CRSwNP_5	53	M	N	Y	N	5	9
Cohort 2							
Control_1	51	M	N	N	N	0	0
Control_2	19	M	N	N	N	0	0
Control_3	17	M	N	N	N	0	0
Control_4	19	M	N	N	N	0	0
Control_5	33	M	N	N	N	0	0
CRSsNP_1	60	M	N	N	Y	2	2
CRSsNP_2	46	M	N	N	N	10	10
CRSsNP_3	54	F	Y	N	Y	8	2
CRSsNP_4	71	M	Y	N	N	8	8
CRSsNP_5	52	F	Y	N	N	12	8
CRSwNP_1	69	F	N	Y	N	8	8
CRSwNP_2	58	M	N	Y	N	8	6
CRSwNP_3	38	M	Y	Y	Y	8	10
CRSwNP_4	35	M	N	Y	N	8	7
CRSwNP_5	54	M	N	Y	N	10	8

L-M score, Lund-Mackay score

Table 2. Demographic characteristics of 99 subjects

Characteristic	Control (n=29)	CRSsNP (n=30)	CRSwNP (n=40)	*P* value*
Male	24 (82.8)	16 (53.3)	27 (67.5)	0.054
Age (yr)	32.4 ± 14.8	41.6 ± 15.1	48.8 ± 14.4	< 0.001
BMI (kg/m^2)	23.3 ± 3.0	23.2 ± 3.4	25.1 ± 4.7	0.171
Smoking	7 (24.1)	4 (13.3)	15 (37.5)	0.072
Atopy	11 (37.9)	7 (24.1)	13 (33.3)	0.515
Polyps	0 (0)	0 (0)	40 (100.0)	< 0.001
Lund-Mackay CT score	0	14.2 ± 6.4	17.3 ± 4.4	< 0.001
Antibiotics†	2 (6.9)	8 (26.7)	16 (40.0)	0.009
Dental problem	1 (3.4)	2 (6.7)	3 (7.5)	0.774
Asthma	0 (0)	2 (6.7)	2 (5.0)	0.397
Allergic rhinitis	13 (44.8)	12 (40.0)	8 (20.0)	0.063
Methodology				
Metagenomic analysis	29	30	40	
Proteomic analysis	23	24	22	

Data are shown as mean ± standard deviation or number (%).

BMI, body mass index; CT, computed tomography.

*P values based on χ^2 or Kruskal-Wallis test (categorical or continuous variables, respectively)

Reagents and materials

Liquid chromatography-mass spectrometry (LC-MS) grade water, methanol, acetonitrile, acetone, and Tris(2-carboxyethyl) phosphine (TCEP) were obtained from Thermo Fisher Scientific (Waltham, USA). Dithiothreitol and urea were purchased from AMRESCO (Solon, USA). Sodium dodecyl sulfate (SDS) and Trizma base were acquired from USB (Cleveland, USA), and sequencing-grade modified trypsin was purchased from Promega Corporation (Madison, USA). POROS20 R2 beads were obtained from Applied Biosystems (Foster City, USA). Unless otherwise noted, all other reagents for proteomic analysis were obtained from Sigma-Aldrich (St. Louis, USA). PowerSoil DNA Isolation Kit for DNA extraction was purchased from Mo Bio Laboratories (Carlsbad, USA).

Preparation of nasal secretions for proteomics

To remove insoluble debris, 100 ml of the aqueous samples were centrifuged at 4℃ (15,000rpm, 10 minutes). Then, the protein concentration in supernatant was determined by tryptophan fluorescence at 350 nm at the excitation of 295nm.[36] The samples were stored at -80℃. The proteins were precipitated using acetone from 50 ml of the aqueous samples (nasal secretions) overnight at -20℃. The proteins were then digested using a modification of the 2-step filter aided sample preparation (FASP) procedure.[37, 38] The pellet was reconstituted with SDT buffer (2% [w/v] SDS, 10 mM TCEP, and 50 mM chloroacetamide in 0.1 M Tris pH 8.0) and filtered through 10K Amicon filters (EMD Millipore, Danvers, USA). After centrifugation at 14,000g, the pellet was resuspended in UA solution (8 M urea in 0.1 M Tris pH 8.5). Subsequently, sample was centrifuged and reconstituted with 40 mM ammonium bicarbonate (ABC). The protein was digested using

trypsin/LysC mixture (protein-to-protease weight ratio of 100:1) overnight at 37°C and the digested peptides were collected via centrifugation. The filters were cleaned with 40 mM ABC, and the digestion was repeated at 37°C for 2 hours (trypsin-to-substrate ratio [w/w] of 1:1,000). The collected peptides were acidified with 10% (v/v) TFA and desalted via C18-StageTips prepared in-house, as previously described.[37, 38] The desalted peptides were lyophilized using vacuum dryer and stored at −80°C.

High-pH StageTip-based peptide fractionation

To establish a spectral library of proteome in nasal secretions, StageTip-based, high-pH peptide fractionation was performed according to modified version of a procedure previously reported.[37] Peptides in pooled samples were reconstituted with 200 ml of loading buffer (10 mM ammonium formate [pH 10] and 2% [v/v] ACN) and separated using reversed-phase tip columns filled with POROS 20 R2 resin (Invitrogen, Carlsbad, USA) into 200μL tips fitted (at the exit sites) with C18 Empore disk membranes (3M, Bracknell, UK). The microcolumn was conditioned with methanol, ACN, and loading buffer and peptides were then loaded at pH 10. Subsequently, twenty fractions were eluted in ACN buffer (pH 10; 5%, 10%, 15%, 20%, 25%, 30%, 35%, 40%, 60%, and 80% [v/v] ACN). To ensure orthogonal fractionation of reverse phase (RP)-RP separation, the twenty fractions were non-contiguously combined into 6 fractions, dried using vacuum centrifuge, and stored at –80°C until LC-MS/MS analysis.

LC-MS/MS analysis

All LC-MS/MS analyses (DDA and DIA) were performed on a Q-Exactive plus

(Thermo Fisher Scientific; Waltham, USA) coupled with an Ultimate 3000 RSLC system (Dionex, Sunnyvale, USA) via a nanoelectrospray source.[39] Peptide samples were separated by a trap (75 µm internal diameter [ID] × 2 cm, C18 3 µm, 100 Å) and analytical column (50 µm ID × 50 cm, C18 1.9 µm, 100 Å). The dried peptide samples were reconstituted with solvent A (2% [v/v] ACN and 0.1% [v/v] formic acid). The samples were then injected into the nano-LC column and eluted with a gradient of 8% to 26% solvent B (100% ACN and 0.1% [v/v] formic acid). The spray voltage and capillary temperature were 2.0 kV (positive ion mode) and 320°C, respectively. In DDA, mass spectra were acquired using a "top 15" method. The Orbitrap analyzer scanned over a mass range 300–1,650 m/z with a mass resolution of 70,000 at 200 m/z. Higher energy collisional dissociation (HCD) scans were collected with a resolution of 17,500 and normalized collision energy (NCE) of 27. The MS/MS scan and maximum ion injection times were 120 and 20 ms, respectively. In DIA, general settings were a resolution of 35,000 (from 400 to 1,220 m/z [automatic gain control target 3×10^6 or injection time 60 ms]). Nineteen DIA windows were acquired at a resolution of 35,000 with an automatic gain of 3×10^6 using the automated injection mode.[40] HCD peptide fragments were collected using 24 to 30 stepped NCE.

Data processing for label-free quantification

The mass spectra were analyzed with MaxQuant software (version 1.5.3.1). MS/MS spectra were searched against the Human Uniprot protein sequence database (December 2014, 88,657 entries) using the Andromeda search engine.[41] Primary searches were performed at a precursor ion tolerance of 6 ppm when total proteins were analyzed. The MS/MS ion tolerance was 20 ppm. Cysteine

carbamidomethylation was set as a fixed modification. N-acetylation and methionine oxidation were set to variable modifications. Enzyme specificity was set to tryptic. Peptides of with least 6 amino acids in length and with up to 2 missed cleavages were analyzed. The false discovery rate (FDR) was set to 0.01 at the peptide, protein and modification levels. The "Match between Runs" in MaxQuant was applied to maximize the number of identified proteins. In silico pools of 5 biological replicates of the same group (control, CRSsNP, and CRSwNP) were generated to minimize heterogeneity between samples,[42] To quantify the proteins in samples, the label-free quantification algorithm[43] was used. The proteins identified from more than 70% of subjects in each group were analyzed .

Data processing for the DIA MS

To generate mass spectral libraries, 12 urine DDA analysis were performed. Then, the spectra were searched with those in the Human Uniprot protein sequence database (December 2014, 88,657 entries) and the indexed retention time (iRT) standard peptide sequences. The mass spectral library (derived from individual the DIA data) was generated by Spectronaut ver. 10 software (Biognosys; Schlieren, Switzerland). First, the DIA raw files were converted into .htrm format using the GTRMS converter of Spectronaut. FDRs were determined using the mProphet[44] approach and were set to 0.01 at both the peptide precursor and protein levels. The protein levels were quantified by the q value < 0.01 criterion. The LC-MS/MS data have been deposited to the Proteome Xchange Consortium via the PRIDE[45] partner repository with the dataset identifier PXD013330 and PXD018960.

DNA extraction and sequencing

For metagenomic analysis, 16S ribosomal DNA (rDNA) in nasal secretions was extracted using the PowerSoil DNA Isolation Kit (Mo Bio Laboratories, Carlsbad, USA) following the manufacturer's instructions. The isolated DNA was amplified and sequences using a Miseq instrument (Illumina, San Diego, USA) in Macrogen Corporation (Macrogen Inc.; Seoul, Korea). Primers 341F (5′-TCG TCG GCA GCG TCA GAT GTG TAT AAG AGA CAG CCT ACG GGN GGC WGC A-3′) and 805R (5′-GTC TCG TGG GCT CGG AGA TGT GTA TAA GAG ACA GGA CTA CHV GGG TAT CTA ATC C-3′) were used to amplify the V3-4 region of 16S rDNA. The 16S rDNA libraries were quantified by TapeStation DNA ScreenTape D1000 (Agilent, Santa Clara, USA) and Picogreen assay. The libraries were sequenced by the MiSeq platform for 2 × 300 cycles. The fastq raw data files have been deposited in the NCBI Sequence Read Archive under BioProject number of PRJNA557492.

Bioinformatics

The protein intensities were transformed to the $\log_2$ scale and missing values were imputed from normal distribution (width = 0.15, downshift = 1.8) using Perseus (version 1.6.0).[46] Then, the data was normalized via width adjustment.[47] Functional gene ontology (GO) analysis was performed using DAVID Bioinformatics Resources ver. 6.8 software (National Institute of Allergy and Infectious Diseases, National Institutes of Health, Bethesda, USA; http://david.abcc.ncifcrf.gov/). The top 10 enriched biological processes were determined using the Enrichr online tool (http://amp.pharm.mssm.edu/Enrichr/).[48] Canonical pathways were identified from the Ingenuity Pathway Analysis (IPA; QIAGEN, Hilden, Germany) software.

Raw sequences were analyzed and quality-filtered with Quantitative Insights Into

Microbial Ecology (QIIME) (version 1.9.1).[49] The sequences were clustered into operational taxonomic units (OTUs) at 97% sequence identity using UCLUST. Taxonomic assignment was then performed SILVA reference database (version 132). To minimize the noise, singletons were excluded from the analysis and 12,634,938 sequences remained. Alpha diversity (Chao1, the number of observed OTUs, Shannon, and Simpson) indices were calculated using the QIIME. To measure beta diversity, principal coordinates analysis (PCoA) was performed with the Bray–Curtis distance matrices using the vegan package in R software (version 3.5.1). Linear discriminant analysis (LDA) effect size (LEfSe) was used to determine differentially abundant families between groups.[50] The relative abundance of each phyla or families was estimated by dividing the read count by the total number of reads in each subject, excluding *Archaea*, *Chloroplast*, and *Mitochondria* reads.

Statistical analysis

The Student's t-test or analysis of variance (ANOVA) was used to evaluate parametric data, while Mann-Whitney U or Kruskal-Wallis tests were used to evaluate non-parametric data. The $\chi 2$ test was used to compare categorical variables between two groups. Pearson's and Spearman's correlation coefficient were calculated for parametric and non-parametric data, respectively. The significance of beta diversity was calculated using permutational multivariate ANOVA (PERMANOVA) using the adonis function in vegan package in R software. LEfSe combines the Kruskal-Wallis or paired Wilcoxon test with linear discriminant analysis. In IPA analysis, the canonical pathways were analyzed using Fisher's exact test with significance at P value < 0.001. Spearman's correlation was

performed to evaluate the correlation and adaptive sum of powered correlation (aSPC) test.[51] It was used to calculate global association between microbiome and proteome. Statistical analyses were performed with SPSS ver. 25.0 (SPSS Inc., Chicago, USA), Perseus (version 1.6.0), and R software (version 3.5.1).

RESULTS

Protein profiles in the DDA set

First, I sought to confirm whether sufficient number of proteins could be obtained from nasal secretions on filter papers. The proteins were detected by LC-MS/MS that has been established as a reliable technique for proteomic analysis.[52] To date, there are two main approaches: data-dependent acquisition (DDA) and data-independent acquisition (DIA).[53] DDA is a traditional approach and peptide signals that are larger than the noise are selected for fragmentation and produce MS/MS spectra.[54] Although it generates high-quality spectra[55], this approach mainly focuses on the most abundant peptides and has poor reproducibility.[53] On the other hand, in Data-independent acquisition (DIA), all peptides within defined mass (m/z) ranges are fragmented and analyzed. It provides accurate peptide quantification and shows better reproducibility than DDA.[54] However, the peptide quantification in DIA is performed using the spectral libraries derived from DDA experiments.[53] So far, there is no conclusion as to which is the best method, and they are complementary to each other. Therefore, to obtain reliable and reproducible results, the proteins were analyzed using both DDA and DIA methods. The workflow was shown in Fig. 1.

First, to investigate the protein profiles of nasal secretions on the filter papers, the nasal secretions from middle meatus of 5 control, 5 CRSsNP, and 5 CRSwNP subjects were analyzed by LC-MS/MS in DDA mode (the DDA set). The mean protein concentration in the DDA set was 1.95 mg/mL (standard deviation [SD], 2.56 mg/mL) in healthy controls, 0.95 mg/mL (SD, 0.84 mg/mL) in CRSsNP

patients and 0.85 mg/mL (SD, 0.49 mg/mL) in CRSwNP subjects, respectively; there was no significant difference between groups ($P = 0.50$).

The number of identified proteins in the set were presented in Fig. 2A. A total of 2,020 proteins was detected in 5 controls, 5 CRSsNP, and 5 CRSwNP subjects (1,745, 1,542, and 1,678 proteins, respectively). Then, I compared the number of proteins identified in nasal secretions collected on filter papers with those of identified in previous proteomic studies of nasal samples (Fig. 2B and Table 3). The number of proteins identified in this study was approximately 3-fold greater than those identified in previous studies.[9, 56-58] Although I attempted to analyze secreted proteome, the number of detected proteins was comparable to that in the nasal epithelium.[42]

To identify the significant GO terms, I performed GO enrichment analysis of 1,842 proteins that were identified in the pooled DDA set using DAVID and revealed 13 biological processes (Fig. 3). The term with the lowest *P* value was immune system processes ($P = 1.51e-41$); the proteome in nasal secretions were thus significantly associated with the immune system. Additionally, to identify the canonical pathways of differentially expressed proteins (DEPs) in CRS, I first detected 924 and 548 DEPs between CRSsNP vs control and CRSwNP vs control in the pooled DDA set, respectively ($P < 0.05$). Then, ingenuity pathway analysis (IPA) was performed on the DEPs and revealed 112 pathways that were significantly enriched (Fig. 4). Among them, I focused on 11 pathways associated with immune system according to Fig.3. CCR3 signaling in eosinophils and IL-17A signaling in airway cells were enriched in both CRSsNP and CRSwNP compared to control. Interferon signaling, coagulation and complement systems were down-regulated in both CRSsNP and CRSwNP.

Hierarchical clustering of DEPs among control, CRSsNP, and CRSwNP in the DDA set

I then identified 1,666 DEPs among control, CRSsNP, and CRSwNP groups to perform a hierarchical cluster analysis (ANOVA, FDR < 0.05) (Fig. 5). Interestingly, the expression pattern of proteins in CRSsNP differed from those in other groups. As polyposis is more severe form of CRS, I investigated the up- or down-regulated DEPs in CRSwNP and revealed 3 clusters; Cluster 1 included 133 proteins with the highest expression in CRSwNP followed by control, Cluster 2 included 294 proteins with down-regulated in CRSwNP and Cluster 3 included 147 proteins with the highest expression in CRSwNP followed by CRSsNP.

The enriched biological processes of up- or down-regulated proteins in CRSwNP

I used the Enrichr software to investigate the GO biological processes and generate the clustergrams. Twenty proteins belonging to the top 10 biological processes indicated that the up-regulated proteins in CRSwNP (Cluster 1 and 3) were significantly associated with neutrophil-related terms (Fig. 6A, C). To confirm this, histology was performed on nasal tissue from CRS patients in the DDA set (Table 4). The set was composed of 2 patients with eosinophilic CRS (CRSsNP_1, 4), 7 with non-eosinophilic CRS, and 1 with unknown (CRSwNP_3). As 4 out of 5 CRSwNP subjects were non-eosinophilic, enriched neutrophil-related terms in CRSwNP could be explained by the histology. On the other hand, the down-regulated proteins in CRSwNP (Cluster 2) were significantly involved in platelet-related terms (Fig. 6B).

Protein profiles in the DIA set

As noted above, although the DDA mode is used to identify thousands of proteins, its reproducibility and precision are restricted.[54] Thus, to obtain reliable and reproducible results on different analytical methods and cohorts, the nasal secretions from the other cohorts (cohort 2) were additionally analyzed in DIA mode (the DIA set). A total of 1,278 proteins were quantified in the DIA set and the number of quantified proteins in each subject was represented in Fig. 7.

Hierarchical clustering of DEPs among control, CRSsNP, and CRSwNP in the DIA set

I then identified 125 DEPs among control, CRSsNP, and CRSwNP groups to perform a hierarchical cluster analysis in the DIA set (ANOVA, FDR < 0.05) (Fig. 8A). As mentioned above, I investigated the up- or down-regulated DEPs in CRSwNP and revealed 2 clusters in the DIA set; Cluster 1 included 61 proteins with down-regulated in CRSwNP and Cluster 2 included 55 proteins with up-regulated in CRSwNP.

The enriched biological processes of commonly up- or down-regulated proteins in CRSwNP

I sought to select the proteins that showed similar expression patterns in both the DDA and DIA set. Among the up-regulated proteins in CRSwNP (Cluster 1 and 3) in the DDA set, I picked out the same proteins were up-regulated in the DIA set (Cluster 2); 10 proteins were detected (Table 5). Similarly, among the down-regulated proteins in CRSwNP (Cluster 2) in the DDA set, I picked out the same

proteins were down-regulated in the DIA set (Cluster 1); 14 proteins were detected (Table 5).

I used the Enrichr software to investigate the GO biological processes and generate the clustergrams (Fig. 8B, C). Interestingly, the up-regulated proteins (ferritin light chain [*FTL*], ferritin heavy chain [*FTH1*], and lysosomal alpha-glucosidase [*GAA*]) and down-regulated proteins (coactosin-like protein [*COTL1*], calmodulin-like protein 5 [*CALML5*], protein S100-A7 [*S100A7*], and eosinophil cationic protein [*ECP*; *RNASE3*]) in CRSwNP were associated with neutrophil-related terms. Meanwhile, the up-regulated proteins were associated with iron-related terms and down-regulated proteins were associated with antimicrobial and peptidase related terms.

Differences in the microbial composition and proteome in relation to disease status

A lot of microorganisms exist in nasal cavity[59] and their dysbiosis could contribute to pathogenesis of CRS.[6, 60] To obtain a better understanding of CRS, nasal epithelial response and environment should be considered together. Thus, I performed integrative analysis to investigate associations between nasal environment and host response. The nasal environment was analyzed by identifying the nasal microbial composition through metagenomics and host response was analyzed by determining the secreted proteome in the nasal cavity through proteomics. The workflow was shown in Fig. 9.

First, I performed metagenomic sequencing on nasal secretions from middle meatus of 29 controls, 30 CRSsNP, and 40 CRSwNP subjects and identified 1,329 OTUs at genus level. To explore whether the microbial composition was

significantly different in relation to disease status, I analyzed the alpha and beta diversity in total subjects. Shannon and Simpson indices were significantly increased across control, CRSsNP, and CRSwNP subjects, while Chao1 and the number of observed OTUs were not significantly different among the groups (Fig. 10A). There were significant differences in microbial composition among the groups (Fig. 10B).

To investigate which taxa were different in relation to disease status, I compared the microbial community structure at phylum and family levels. Among taxa with relative abundance >3%, *Firmicutes* and *Bacteroidetes* were significantly increased across control, CRSsNP, and CRSwNP subjects, while *Cyanobacteria* levels were significantly decreased across control, CRSsNP, and CRSwNP subjects (Fig. 11A, C). At the family level, *Staphylococcaceae*, *Propionibacteriaceae*, and *Moraxellaceae* were significantly decreased across control, CRSsNP, and CRSwNP subjects (Fig. 11B, D). *Prevotellaceae* was significantly increased across control, CRSsNP, and CRSwNP subjects. Among all identified families, *Propionibacteriaceae* and *Moraxellaceae* were the most abundant in control, and *Entomoplasmataceae* was the most abundant in CRSsNP subjects (Fig. 11E).

Next, proteomic analysis was performed using the nasal secretions from the same individual analyzed by metagenomics. Among 99 subjects, nasal secretions from 69 subjects (23 control, 24 CRSsNP, and 22 CRSwNP) were available for proteomic analysis. A total number of 2,162 proteins were quantified and the average number was approximately 1,440 proteins. The number of quantified proteins from each subject is shown in Fig. 12A. When comparing control to CRSsNP groups, relatively small proteome changes were observed compared to other comparisons (Fig. 12B and Table 6).

Given that cells could interact with surrounding environment, I hypothesized that the secreted proteome and microbiome could correlate with each other. As mentioned above, I was interested in investigating the up- or down-regulated microbiome and proteins in CRSwNP compared to control and CRSsNP. To examine the hypothesis, I divided the nasal microbiome and proteins into 2 groups, respectively. IFc group included families were significantly increased across control, CRSsNP, and CRSwNP subjects and DFc group included families were significantly decreased across control, CRSsNP, and CRSwNP subjects (Kruskal-Wallis, $P < 0.05$). IPc group included proteins were significantly increased across control, CRSsNP, and CRSwNP subjects and DPc group included proteins were significantly decreased across control, CRSsNP, and CRSwNP subjects (ANOVA, $P < 0.05$). According to GO molecular functions, IPc group were associated with cadherin binding (Table 7). On the other hand, DPc group were associated with cholesterol transfer activity, transition metal ion binding and apolipoprotein receptor binding. After that, I performed correlation analysis among the four groups (Fig. 13A). Furthermore, to evaluate the associations, I used aSPC tests. These analyses uncovered significant global association between IFc and DPc, DFc and IPc, DFc and DPc (aSPC test, $P < 0.01$) (Fig. 13B). These findings suggest a strong association between the nasal microbiome and secreted proteome in relation to disease status.

Differences in the microbial composition and proteome in relation to the use of antibiotics

To identify the effects of antibiotics on the nasal microbiome and host responses, the subjects were divided on whether they had taken antibiotics 3 months prior to

sampling (ABX and NABX, respectively). I then investigated microbial community and secreted proteome. The ABX group comprised of 2 controls, 8 CRSsNP, and 16 CRSwNP subjects, while the NABX group comprised of 27 controls, 22 CRSsNP, and 24 CRSwNP subjects. In the NABX group, unlike Chao1 and the number of observed OTUs, the Shannon and Simpson indices were significantly increased across control, CRSsNP, and CRSwNP subjects (Fig. 14A). There were significant differences in microbial composition among the groups (Fig. 14C). However, in the ABX group, there was no significant difference in the alpha and beta diversities (Fig. 14B, D).

To investigate which taxa were different in relation to disease status, I compared the microbial community structure at the phylum and family levels in the NABX and ABX groups. Among families with relative abundance >3%, in the NABX group, *Firmicute*, *Cyanobacteria*, and *Bacteroidetes* significantly differed in relation to disease status (Fig. 15A, E). At the family level, the relative abundance of *Propionibacteriaceae*, *Moraxellaceae*, and *Prevotellaceae* significantly differed in relation to disease status (Fig. 15B, F). Among all identified families, LEfSe analysis showed that *Propionibacteriaceae* was significantly decreased in CRSwNP and CRSsNP subjects compared to control (Fig. 15G). On the other hand, in the ABX group, there was no significant difference in phyla and families with relative abundance >3% (Fig. 15C, D). Among all detected families, I identified that *Peptostreptococcaceae*, *Desulfovibrionaceae*, and *Alteromonadaceae* were significantly increased in control (Fig. 15H). *Sulfurovaceae* was found to be significantly dominant in CRSsNP subjects. Taken together, these findings implied that the use of antibiotics could reduce differences in microbial community in relation to disease status.

To examine the differences in the microbial community in relation to antibiotic use, I first compared alpha diversity between the NABX and ABX groups in each disease status. Shannon and Simpson indices significantly differed only in CRSwNP subjects (Fig. 16). There was no difference in Chao1 and the number of observed OTUs between the NABX and ABX groups in each disease status (Fig. 17A, 18A, 19A, 20A).

In a total of 99 subjects, PERMANOVA revealed that there were significant differences in microbial composition between the NABX and ABX groups (Fig. 17B). Among families with relative abundance >3%, *Staphylococcaceae*, *Propionibacteriaceae*, and *Streptococcaceae* significantly differed between the two groups (Fig. 17C). Among all identified families, I found that *Staphylococcaceae*, *Streptococcaceae*, and *Propionibacteriaceae* were significantly dominant in the NABX group (Fig. 17D). *Entotheonellaceae* and *Sandaracinaceae* were significantly increased in the ABX group. Then, in control subjects, the beta diversities did not significantly differ between the 2 groups (Fig. 18B). Additionally, there was no significant difference in families with relative abundance >3% (Fig. 18C). Among all identified families, LEfSe analysis revealed that the use of antibiotics contributed to the enrichment of families with relative abundance <3% (Fig. 18D). In CRSsNP subjects, the microbial composition did not significantly differ between the NABX and ABX groups (Fig. 19B). Among families with relative abundance >3%, *Staphylococcaceae* was significantly decreased in the ABX group (Fig. 19C). LEfSe analysis that was performed on all identified families revealed that *Staphylococcaceae*, *Intrasporangiaceae*, and *Neisseriaceae* were significantly enriched in the NABX group (Fig. 19D). Additionally, *Prevotellaceae* and *Legionellaceae* were significantly dominant in the ABX group.

Lastly, the microbial communities were compared between the NABX and ABX groups in CRSwNP subjects. PERMANOVA showed significant differences in microbial composition between the 2 groups (Fig. 20B). Among families with relative abundance >3%, *Streptococcaceae* and *Lachnospiraceae* were significantly enriched in the NABX group (Fig. 20C). Among all detected families, *Streptococcaceae*, *Lachnospiraceae*, and *Neisseriaceae* were significantly dominant in the NABX group (Fig. 20D). According to alpha and beta diversity, it seemed that antibiotics exerted stronger effects on the microbial community in CRSwNP subjects than that in the control and CRSsNP subjects.

Next, I sought to analyze responses of host to antibiotics using proteomic analysis in the non-NP group which consisted of control and CRSsNP subjects and the NP group which consisted of CRSwNP subjects. In the ABX group, relatively small proteome changes were identified between the non-NP and NP groups compared to those in the NABX group (Fig. 21A and Table 8). It was consistent with previous results that the use of antibiotics reduced differences in microbial communities in relation to disease status (Fig. 14, 15).

Furthermore, to determine differences in the secreted proteome in relation to antibiotic use, I compared DEPs ($|\log_2(\text{fold change})| \geq 1.0$ and $P < 0.05$) between the NABX and ABX groups in total of subjects, the non-NP and NP groups, respectively (Fig. 21B and Table 9). As with previous results in Fig. 16, antibiotics also exerted stronger effects on the secreted proteome in the NP group compared to that in total and the non-NP group. I then sought to identify the canonical pathways which were significantly enriched by DEPs between the NABX and ABX groups. In a total of 99 subjects, B cell receptor signaling, P70S6K signaling were significantly increased in the ABX groups (Fig. 21C). On the other hand, in the NP

group, LXL/RXR activation, innate immunity, and production nitric oxide (NO) and reactive oxygen species (ROS) were significantly enriched in the ABX group (Fig. 21D). There was no significant pathway found in the non-NP group ($P > 0.001$). Taken together, these analyses revealed that the use of antibiotics might have stronger effects on nasal microbiome and host responses in CRSwNP compared to those in control and CRSsNP subjects.

Antibiotic-dependent relationships between nasal microbiome and secreted proteome

I then sought to examine whether the associations between the microbiome and secreted proteome could be varied in relation to antibiotic use. The associations with a large number of significant correlations between microbiome and proteins were considered as meaningful. Thus, I arranged the microbiome and secreted proteome in descending order from the largest number of significant correlations between each other, respectively. Next, the top 25 percent of the families and secreted proteins were selected, respectively, and hierarchical clustered (Fig. 22A, B). The average R-squared value in the ABX was larger than that in the NABX group. From these results, I confirmed that the correlation between the families and secreted proteins in the ABX group was strengthened compared to those observed in the NABX group. Likewise, the associations between the microbiome and secreted proteome could be altered in relation to the use of antibiotics. In addition, the correlation between them was strengthened in subjects who had taken antibiotics.

Antibiotic-dependent relationships between the nasal microbiome and secreted proteome in the non-NP and NP groups

Finally, given that antibiotics exerted different effects on the nasal microbiome and secreted proteome in relation to disease status, I hypothesized that the associations between microbiome and proteins that were increased or decreased in the ABX group could differ in relation to disease status. To examine the hypothesis, I divided the nasal microbiome and proteins into 2 groups, respectively. IFa group included families were significantly increased in the ABX group and DFa group included families were significantly decreased in the ABX group (Mann-Whitney U test, $P < 0.05$). IPa group included proteins were significantly increased in the ABX group and DPa group included proteins were significantly decreased in the ABX group (Student's t-test, $P < 0.05$). After that, I performed correlation analysis among the four groups (Fig. 23A, B). Furthermore, to evaluate the associations, I used aSPC tests (Fig. 23C). The associations between DFa and IPa, DFa and DPa in the NP group were more significant than those in the non-NP group. Therefore, the association between the nasal microbiome and secreted proteome was stronger in CRSwNP than in control and CRSsNP.

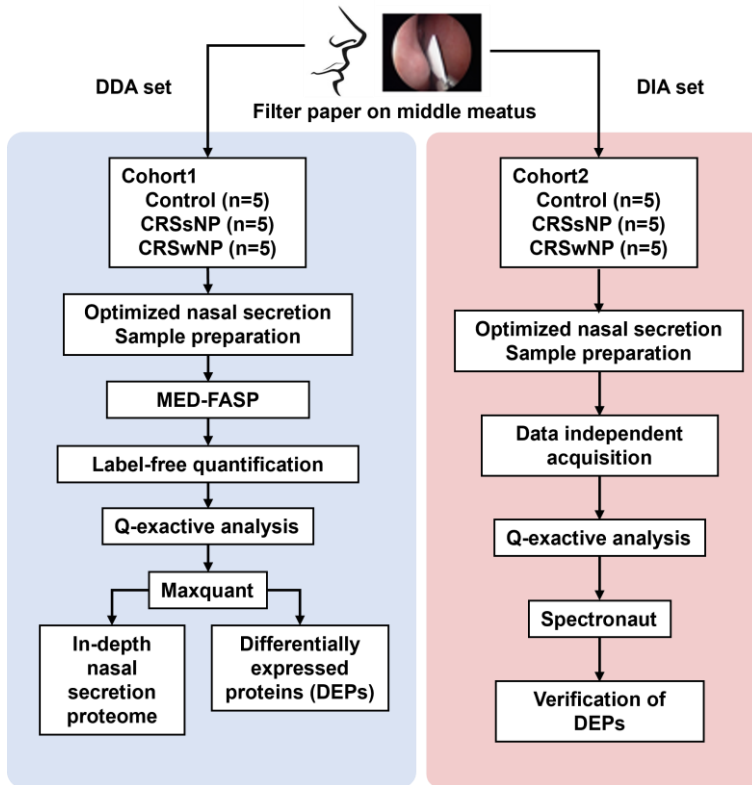

Figure 1. Workflow of proteomic analysis

MED-FASP, multi-enzyme digestion filter aided sample preparation.

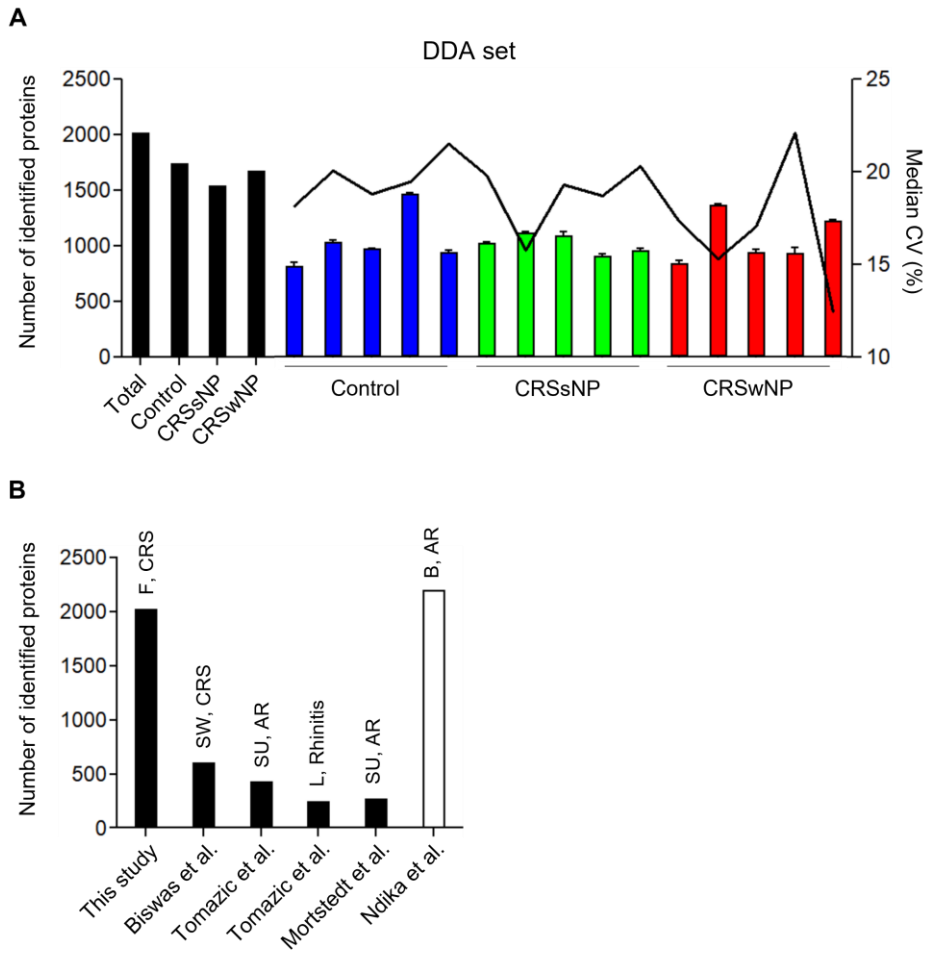

Figure 2. Proteome profiles in the DDA set

(A) Total number of the identified proteins from technical triplicates in the DDA set (Error bars = mean ± standard deviations of triplicates). (B) The plot showing the comparison of the identified proteins in this study and previous proteomic studies of nasal samples.

F, filter papers; SW, swab; SU, suction; L, nasal lavage; B, brushing; AR, allergic rhinitis.

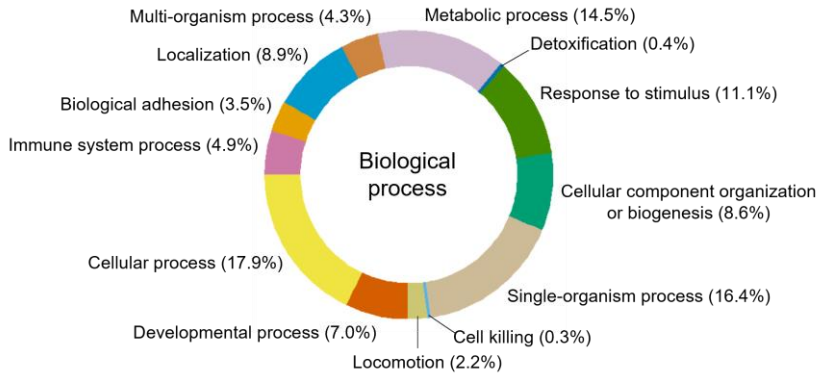

Figure 3. Functional gene ontology (GO) of proteome in nasal secretions

Donut chart showing the significant GO biological processes of the proteome ($P < 0.05$). The terms were arranged in order of *P* value from smallest to largest (the pathway with the lowest *P* value was immune system process and with the largest was the cellular process). The percentage of the number of proteins associated with each term was indicated in parenthesis.

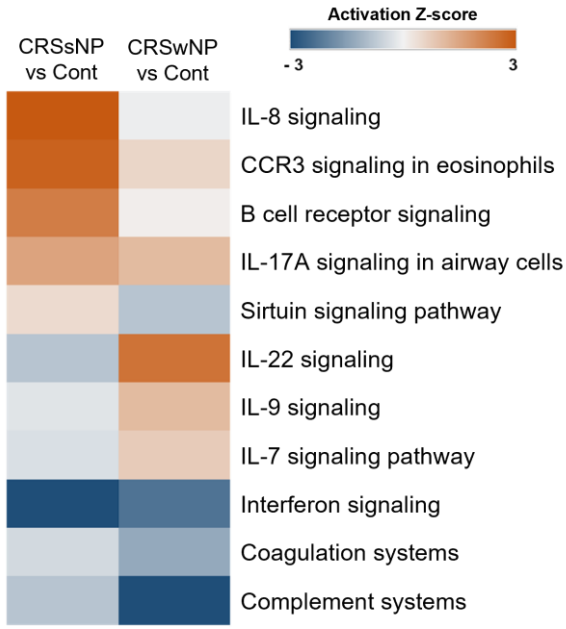

Figure 4. Canoncal pathway analysis of the significantly up- or down-regulated proteins in CRSsNP and CRSwNP compared to control

The pathways arranged in order of the highest to lowest z-score. The positive and negative scores represented in orange and blue, respectively.

Cont, control; IL, interleukin; CCR3, C-C chemokine receptor type 3.

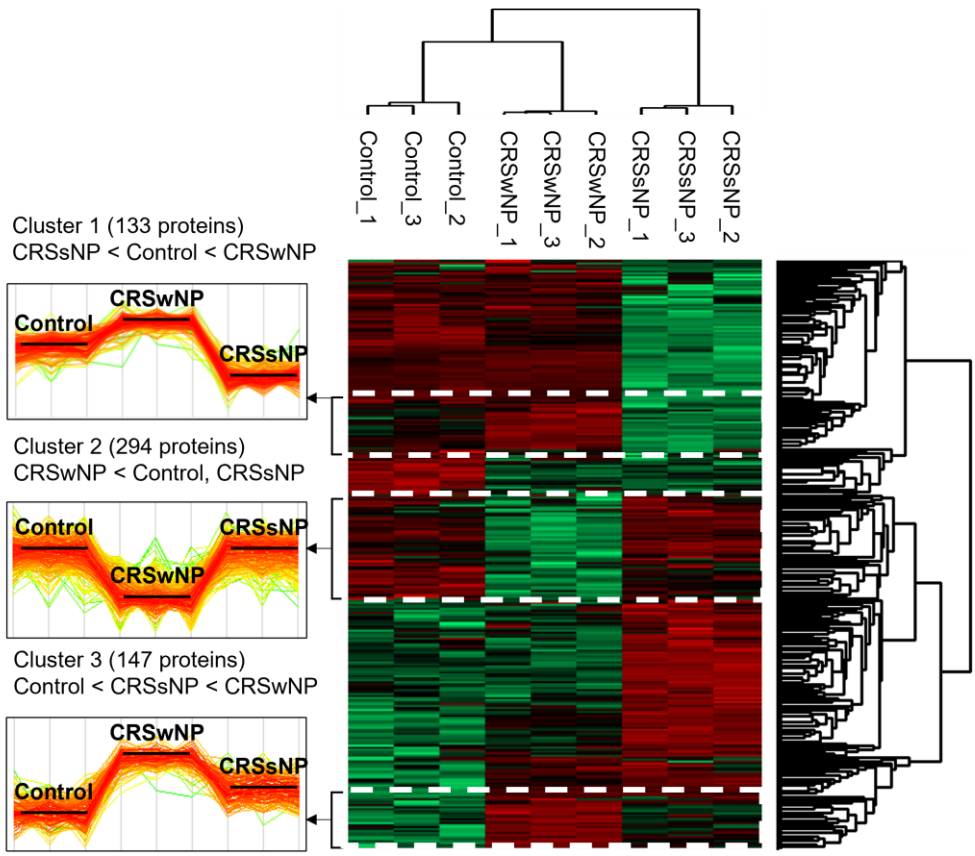

Figure 5. Hierarchical clustering of DEPs in the DDA set

A heatmap of total number of 1,666 proteins identified as DEPs (ANOVA, FDR < 0.05).

Figure 6. Biological processes of up- or down-regulated proteins in CRSwNP

The clustergrams illustrating the top 10 enriched terms and twenty proteins associated with those terms in Cluster 1 (A), Cluster 2 (B), and Cluster 3 (C), respectively. The rows represented the top 10 enriched terms ranked by their enrichment score, and the columns represented the weighted input genes were hierarchically clustered based on their association with columns.

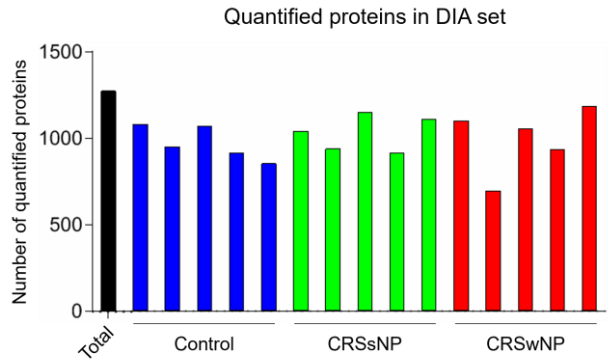

Figure 7. Quantified proteome in the DIA set

A total of 1,278 proteins quantified in technical duplicates in the DIA set.

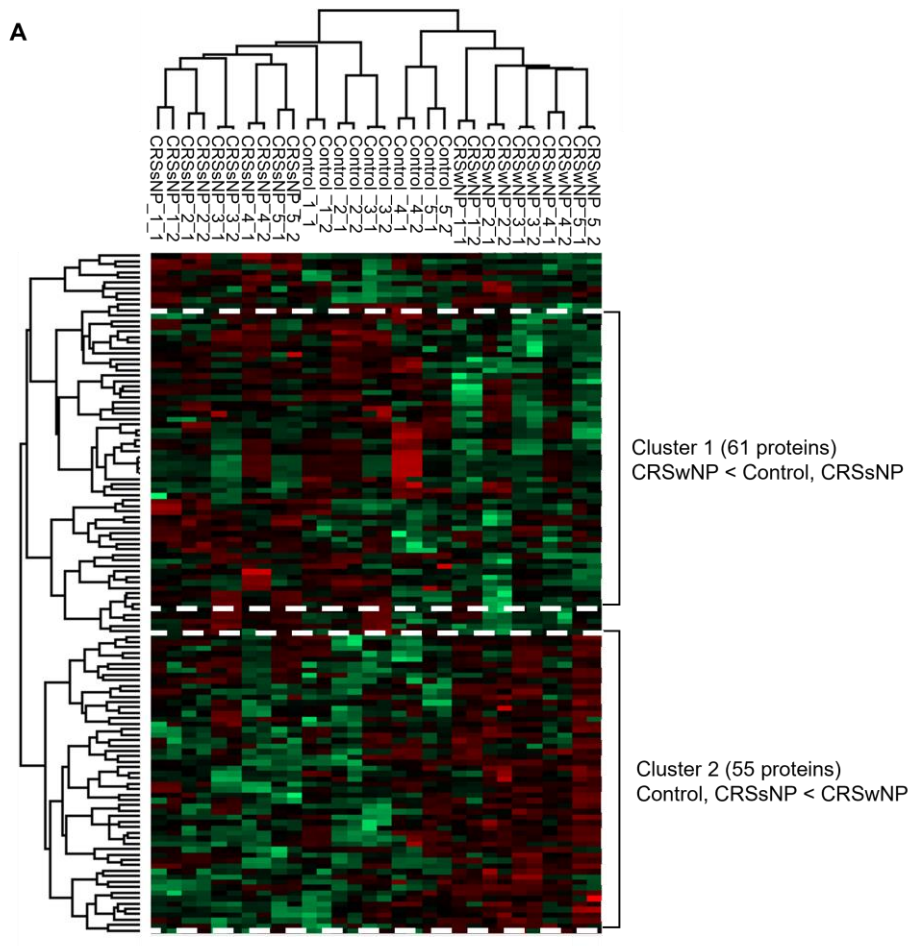

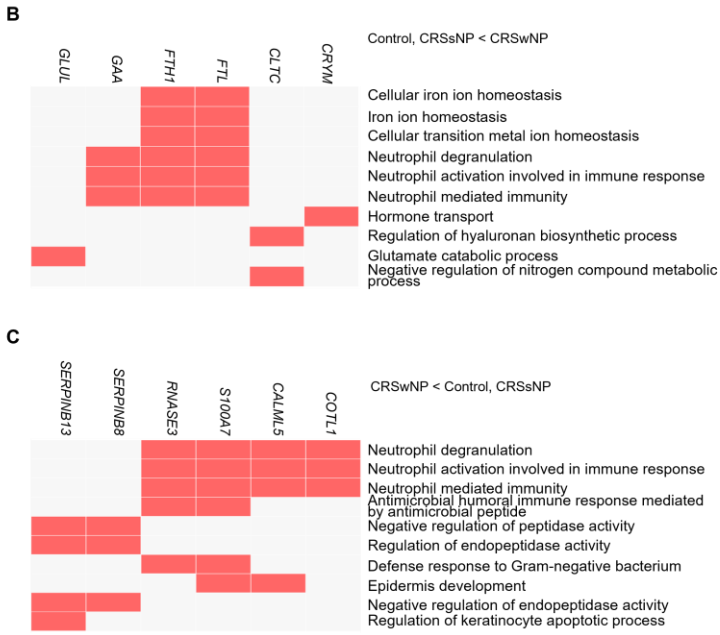

Figure 8. Verification of DEPs in CRSwNP

(A) A heatmap and hierarchical clustering of total number of 125 proteins identified as DEPs in the DIA set (ANOVA, FDR < 0.05). Biological processes of up- (B) or down-regulated (C) proteins in CRSwNP both in the DDA and DIA set. The top 10 enriched terms and proteins associated with those terms were illustrated. The rows represented the top 10 enriched terms ranked by their enrichment score, and the columns represented the weighted input genes were hierarchically clustered based on their association with columns.

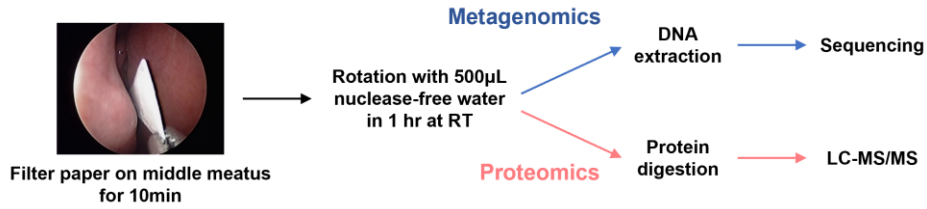

Figure 9. Workflow of metagenomic and proteomic analysis

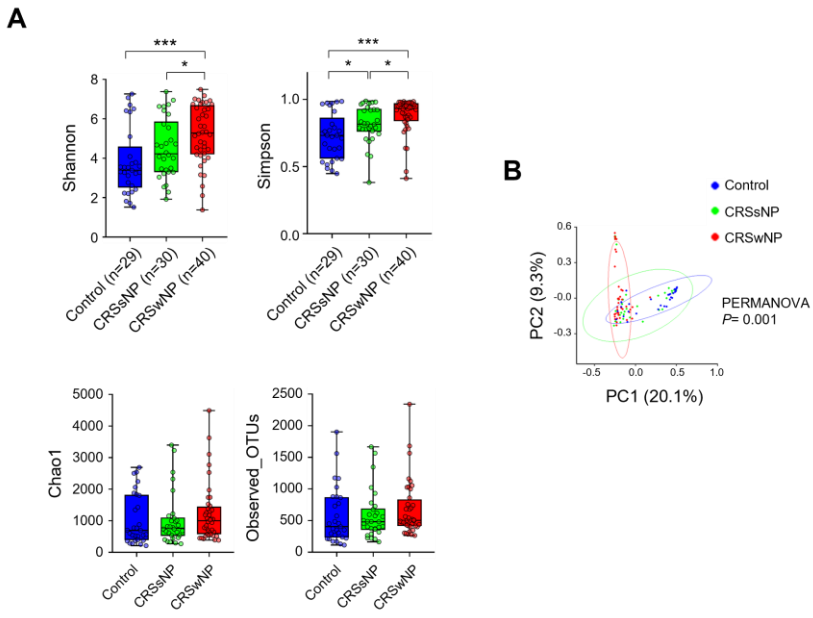

Figure 10. Diversity of nasal microbiome in relation to disease status

Comparison of alpha diversity among control, CRSsNP, and CRSwNP (horizontal line = median and whiskers = min and max values). (B) Principal coordinates analysis (PCoA) using Bray-Curtis distance matrix.

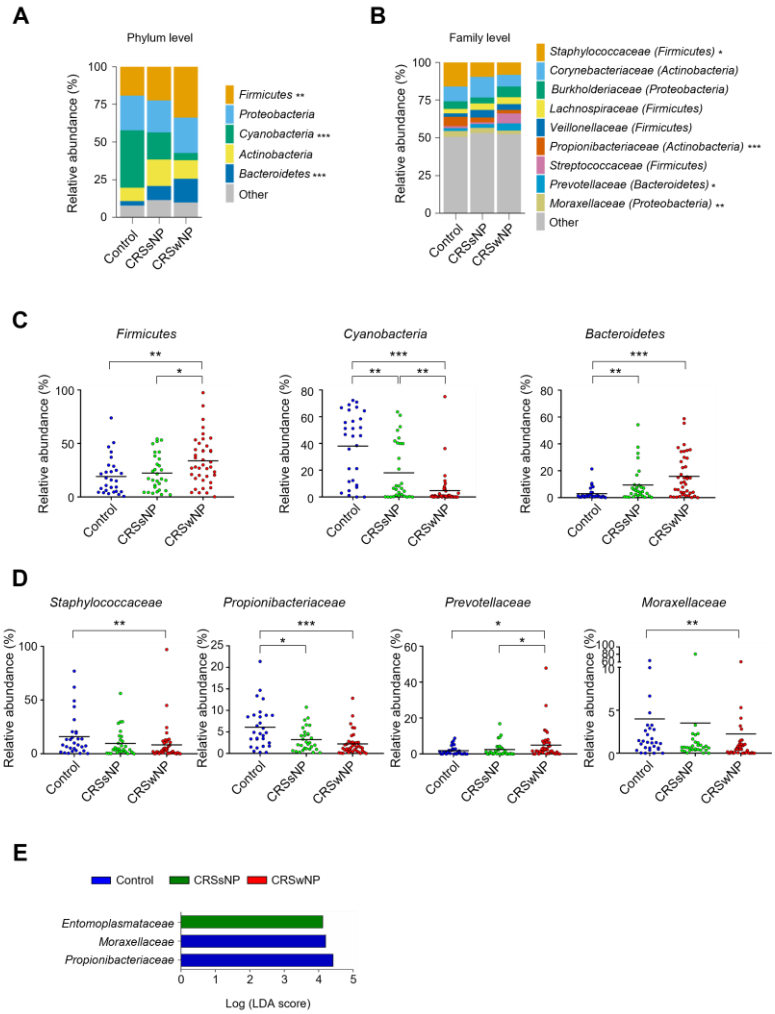

Figure 11. Nasal microbiome composition in relation to disease status

The distribution of microbiome at phylum (A) and family (B) level. The stacked bar plots showed the composition of phyla or families with relative abundance greater than three percent. The plots represented the phyla (C) and families (D) with significantly different relative abundance between disease status. (E) Linear discriminant analysis effect size (LEfSe) analysis with LDA score > 3.0 and *P* value < 0.05 in all-against-all (more stringent). Control, CRSsNP, and CRSwNP enriched families were colored in blue, green, and red, respectively.

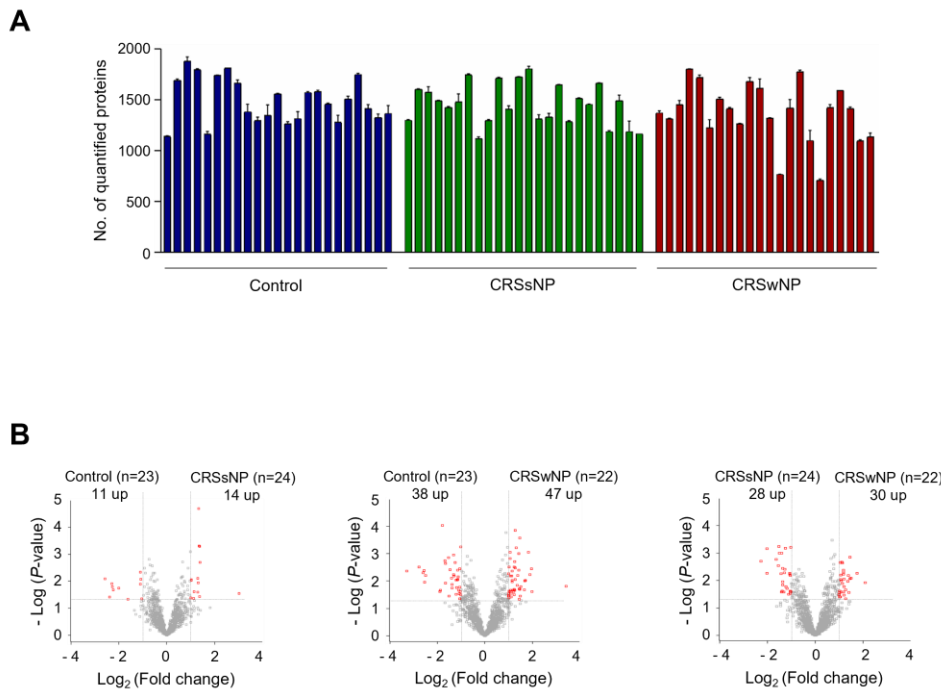

Figure 12. Proteome profiles in nasal secretions

A total of 2,162 proteins were quantified in technical duplicates (Error bars = mean ± standard deviations of duplicates). (B) Volcano plots indicated the $\log_2$ fold change against the negative $\log_{10}$ of *P* value between control, CRSsNP, and CRSwNP. The horizontal dashed line represented *P* value of 0.05, and the vertical dashed lines represented with | $\log_2$ (fold change) | of 1.0. Red squares illustrated proteins with | $\log_2$ (fold change) | ≥ 1.0 and *P* value < 0.05.

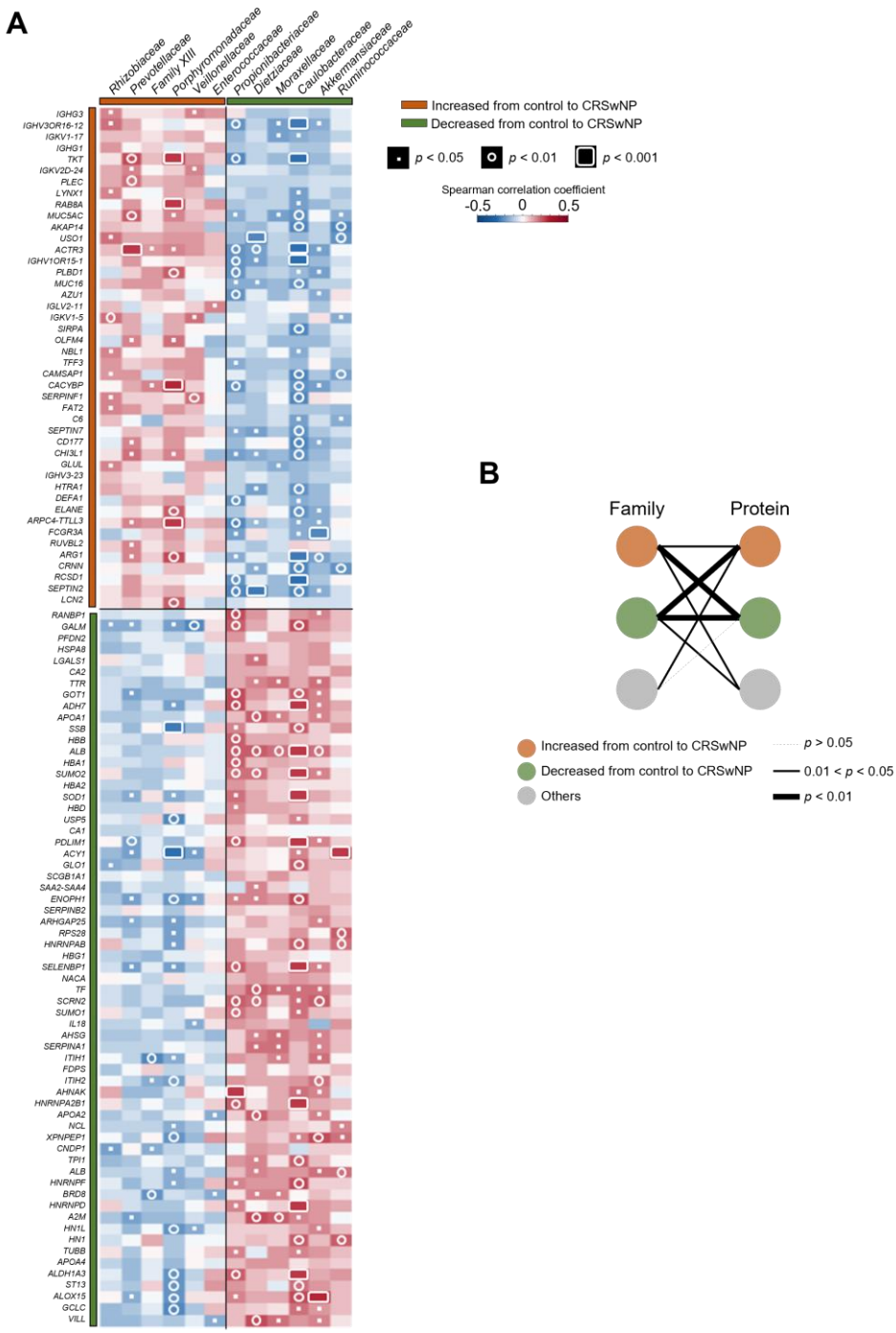
A
Rhizobiaceae
Prevotellaceae
Family XIII
Porphyromonadaceae
Veillonellaceae
Enterococcaceae
Propionibacteriaceae
Dietziaceae
Moraxellaceae
Caulobacteraceae
Akkermansiaceae
Ruminococcaceae
IGHG3
IGHV3OR16-12
IGKV1-17
IGHG1
TKT
IGKV2D-24
PLEC
LYNX1
RABBA
MUC5AC
AKAP14
USO1
ACTR3
IGHV1OR15-1
PLBD1
MUC16
AZU1
IGLV2-11
IGKV1-5
SIRPA
OLFM4
NBL1
TFF3
CAMSAP1
CACYBP
SERPINF1
FAT2
C6
SEPTIN7
CD177
CHI3L1
GLUL
IGHV3-23
HTRA1
DEFA1
ELANE
ARPC4-TTLL3
FCGR3A
RUVBL2
ARG1
CRNN
RCSD1
SEPTIN2
LCN2
RANBP1
GALM
PFDN2
HSPA8
LGALS1
CA2
TTR
GOT1
ADH7
APOA1
SSB
HBB
ALB
HBA1
SUMO2
HBA2
SOD1
HBD
USP5
CA1
PDLIM1
ACY1
GLO1
SCGB1A1
SAA2-SAA4
ENOPH1
SERPINB2
ARHGAP25
RPS28
HNRNPAB
HBG1
SELENBP1
NACA
TF
SCRN2
SUMO1
IL18
AHSG
SERPINA1
ITIH1
FDPS
ITIH2
AHNAK
HNRNPA2B1
APOA2
NCL
XPNPEP1
CNDP1
TPI1
ALB
HNRNPF
BRD8
HNRNPD
A2M
HN1L
HN1
TUBB
APOA4
ALDH1A3
ST13
ALOX15
GCLC
VILL
Increased from control to CRSwNP
Decreased from control to CRSwNP
p < 0.05
p < 0.01
p < 0.001
Spearman correlation coefficient
-0.5
0
0.5
B
Family
Protein
Increased from control to CRSwNP
Decreased from control to CRSwNP
Others
p > 0.05
0.01 < p < 0.05
p < 0.01

Figure 13. Correlation between up- or down-regulated families and proteins in CRSwNP

A heatmap of the secreted proteins (ANOVA, $P < 0.05$) and families (Kruskal-Wallis, $P < 0.05$). The proteins and families were ordered from top to bottom and from left to right in order of lowest to highest *P* value, respectively. Orange and green colors represented significantly increased and decreased families or proteins, respectively, from control to CRSwNP. Redundant microbiome and proteins were ruled out. (B) Association between families and proteins were significantly increased or decreased from control to CRSwNP (aSPC test, $P < 0.05$). Orange and green colors indicated the same groups previously described in (A). Families and proteins were not included in the orange and green colors were considered as Others (colored in gray).

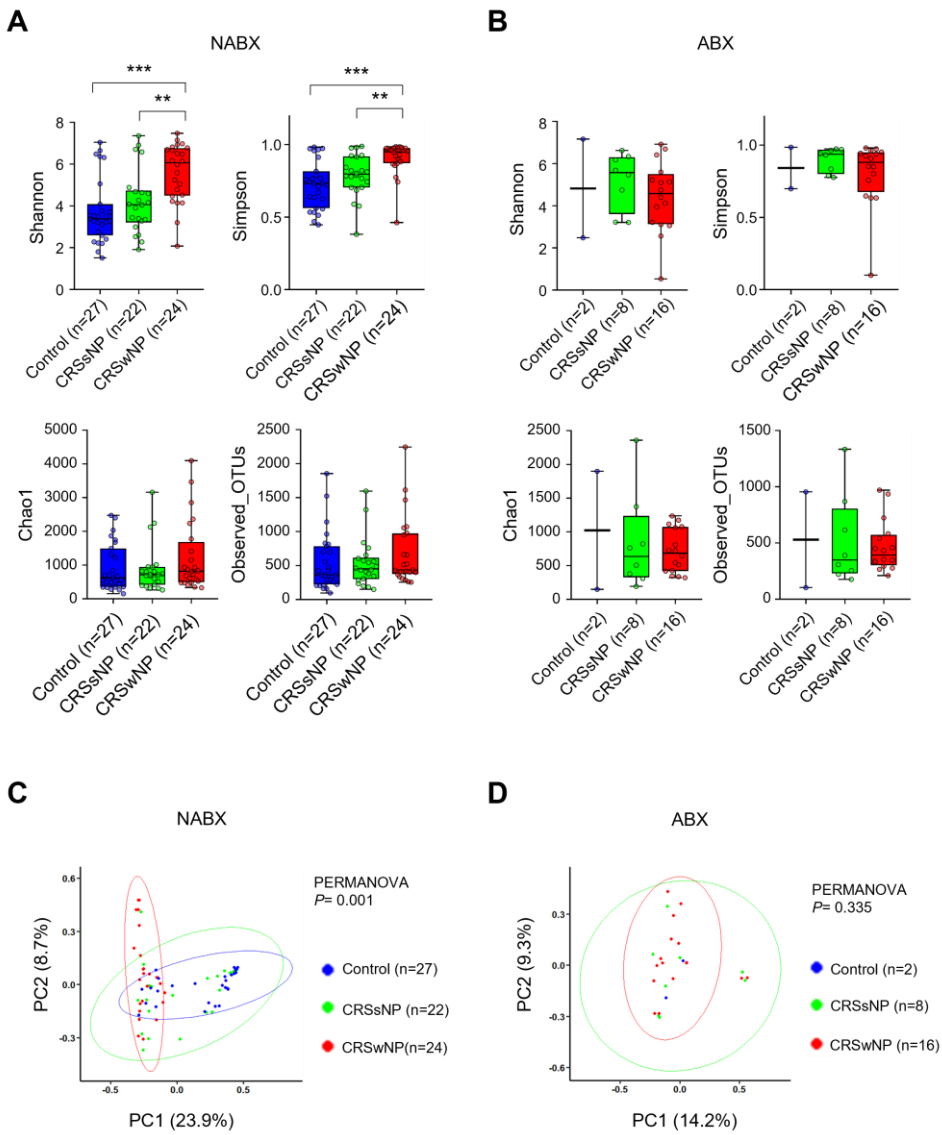

Figure 14. Diversity of nasal microbiome in relation to the use of antibiotics

Alpha diversity in relation to disease status in the NABX (A) and ABX (B) groups (horizontal line = median and whiskers = min and max values). Principal coordinates analysis (PCoA) using Bray-Curtis distance matrix in the NABX (C) and ABX (D) groups.

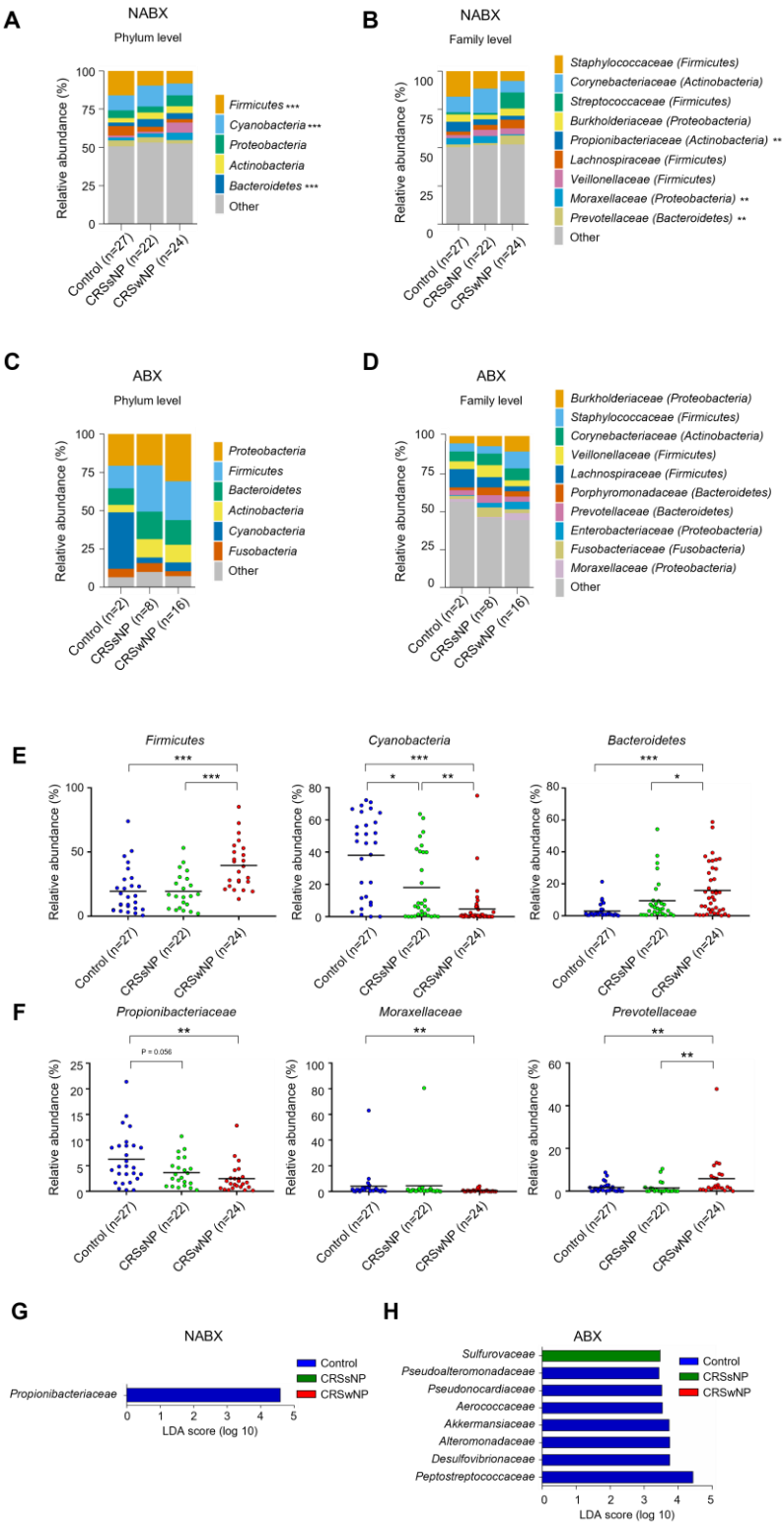
A
NABX
Phylum level
Relative abundance (%)
Firmicutes ***
Cyanobacteria ***
Proteobacteria
Actinobacteria
Bacteroidetes ***
Other
Control (n=27)
CRSsNP (n=22)
CRSwNP (n=24)
B
NABX
Family level
Staphylococcaceae (Firmicutes)
Corynebacteriaceae (Actinobacteria)
Streptococcaceae (Firmicutes)
Burkholderiaceae (Proteobacteria)
Propionibacteriaceae (Actinobacteria) **
Lachnospiraceae (Firmicutes)
Veillonellaceae (Firmicutes)
Moraxellaceae (Proteobacteria) **
Prevotellaceae (Bacteroidetes) **
Other
C
ABX
Phylum level
Proteobacteria
Firmicutes
Bacteroidetes
Actinobacteria
Cyanobacteria
Fusobacteria
Other
Control (n=2)
CRSsNP (n=8)
CRSwNP (n=16)
D
ABX
Family level
Burkholderiaceae (Proteobacteria)
Staphylococcaceae (Firmicutes)
Corynebacteriaceae (Actinobacteria)
Veillonellaceae (Firmicutes)
Lachnospiraceae (Firmicutes)
Porphyromonadaceae (Bacteroidetes)
Prevotellaceae (Bacteroidetes)
Enterobacteriaceae (Proteobacteria)
Fusobacteriaceae (Fusobacteria)
Moraxellaceae (Proteobacteria)
Other
E
Firmicutes
Cyanobacteria
Bacteroidetes
F
Propionibacteriaceae
P = 0.056
Moraxellaceae
Prevotellaceae
G
NABX
Propionibacteriaceae
Control
CRSsNP
CRSwNP
LDA score (log 10)
H
ABX
Sulfurovaceae
Pseudoalteromonadaceae
Pseudonocardiaceae
Aerococcaceae
Akkermansiaceae
Alteromonadaceae
Desulfovibrionaceae
Peptostreptococcaceae
Control
CRSsNP
CRSwNP
LDA score (log 10)

Figure 15. Nasal microbiome composition in relation to the use of antibiotics

The distribution of microbiome at phylum (A, C) and family (B, D) level. The stacked bar plots showed the composition of phyla or families with relative abundance greater than three percent. The plots represented the phyla (E) and families (F) with significantly different relative abundance between disease status in the NABX group. Linear discriminant analysis effect size (LEfSe) analysis with LDA score > 3.0 and *P* value < 0.05 in all-against-all (more stringent) in the NABX (G) and ABX (H) groups. Control, CRSsNP, and CRSwNP enriched families were colored in blue, green, and red, respectively.

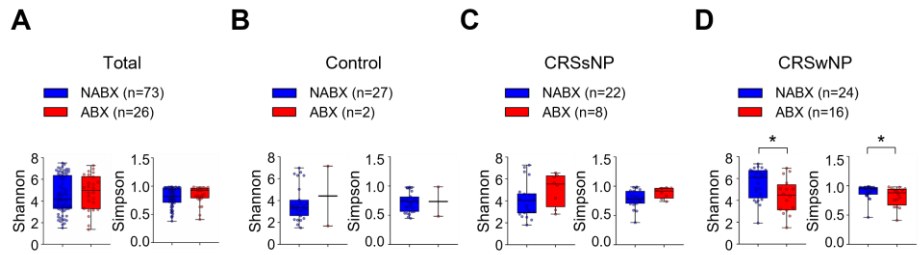

Figure 16. Comparison of alpha diversity of nasal microbiome between the NABX and ABX groups

Shannon and Simpson indices between the NABX and ABX groups in a total of 99 subjects (A), control (B), CRSsNP (C), and CRSwNP (D), respectively (horizontal line = median and whiskers = min and max values).

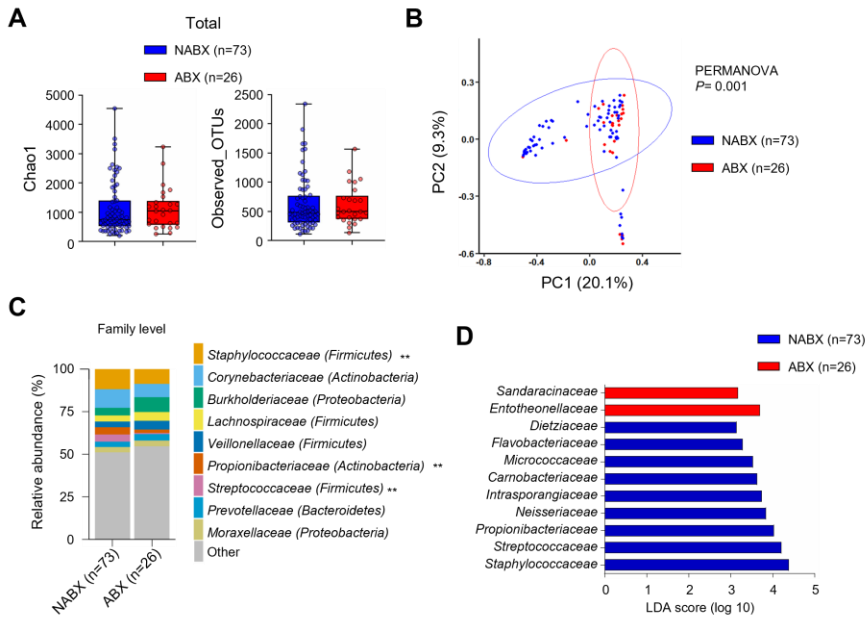

Figure 17. Microbial differences in relation to the use of antibiotics in total of 99 subjects

(A) Chao1 and observed OTUs indices between the NABX and ABX groups in a total of 99 subjects (horizontal line = median and whiskers = min and max values). (B) Principal coordinates analysis (PCoA) using Bray-Curtis distance matrix. (C) The distribution of microbiome at family level. The stacked bar plots showed the composition of families with relative abundance greater than three percent. (D) Linear discriminant analysis effect size (LEfSe) analysis with LDA score > 3.0 and *P* value < 0.05 in all-against-all (more stringent). NABX and ABX enriched families were colored in blue and red, respectively.

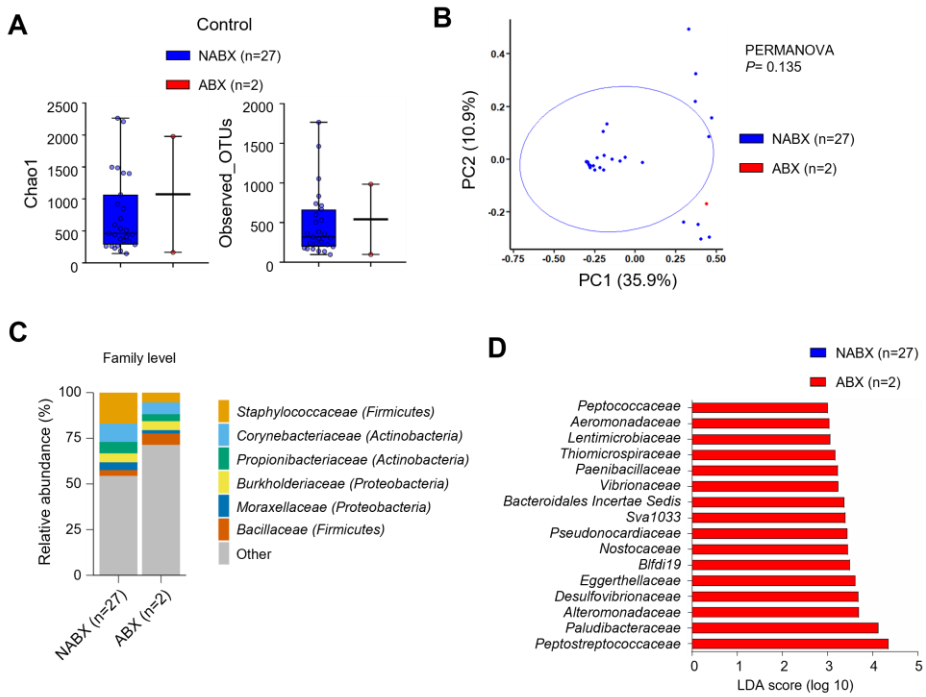

Figure 18. Microbial differences in relation to the use of antibiotics in control

(A) Chao1 and observed OTUs indices between the NABX and ABX groups in control group (horizontal line = median and whiskers = min and max values). (B) Principal coordinates analysis (PCoA) using Bray-Curtis distance matrix. (C) The distribution of microbiome at family level. The stacked bar plots showed the composition of families with relative abundance greater than three percent. (D) Linear discriminant analysis effect size (LEfSe) analysis with LDA score > 3.0 and *P* value < 0.05 in all-against-all (more stringent). NABX and ABX enriched families were colored in blue and red, respectively.

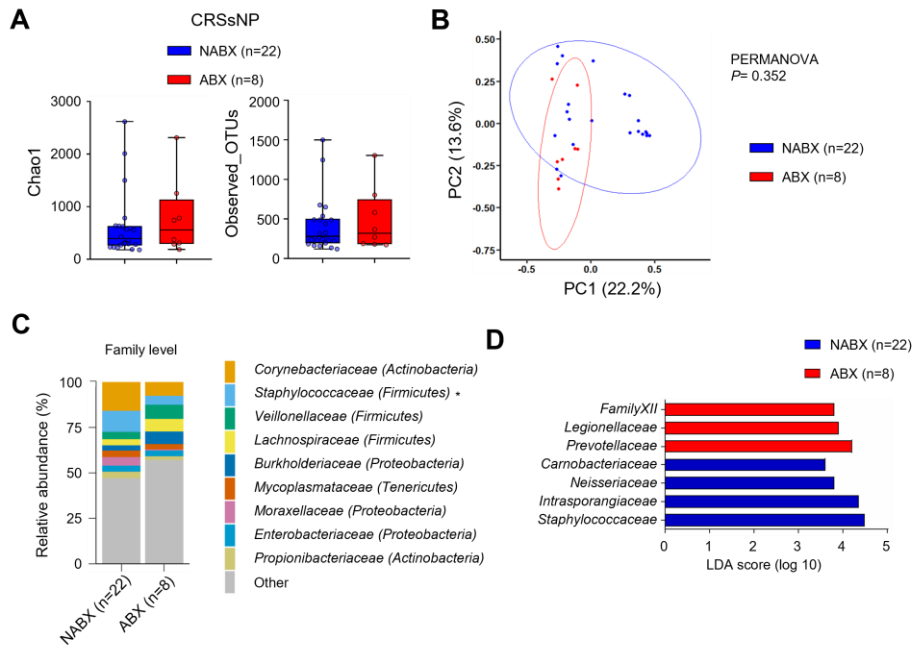

Figure 19. Microbial differences in relation to the use of antibiotics in CRSsNP

(A) Chao1 and observed OTUs indices between the NABX and ABX groups in CRSsNP patients (horizontal line = median and whiskers = min and max values). (B) Principal coordinates analysis (PCoA) using Bray-Curtis distance matrix. (C) The distribution of microbiome at family level. The stacked bar plots showed the composition of families with relative abundance greater than three percent. (D) Linear discriminant analysis effect size (LEfSe) analysis with LDA score > 3.0 and *P* value < 0.05 in all-against-all (more stringent). NABX and ABX enriched families were colored in blue and red, respectively.

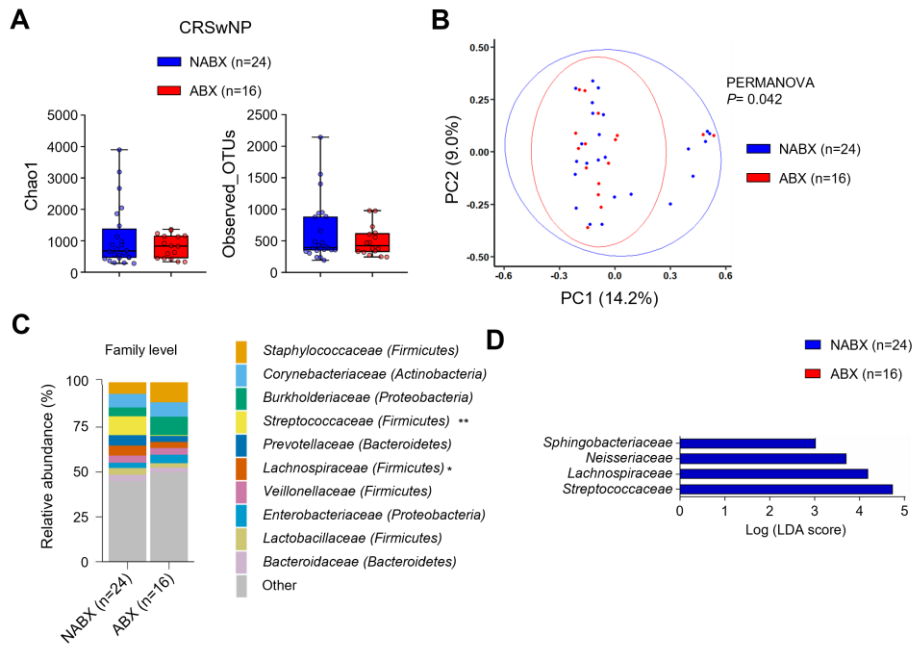

Figure 20. Microbial differences in relation to the use of antibiotics in CRSwNP

(A) Chao1 and observed OTUs indices between the NABX and ABX groups in CRSwNP patients (horizontal line = median and whiskers = min and max values). (B) Principal coordinates analysis (PCoA) using Bray-Curtis distance matrix. (C) The distribution of microbiome at family level. The stacked bar plots showed the composition of families with relative abundance greater than three percent. (D) Linear discriminant analysis effect size (LEfSe) analysis with LDA score > 3.0 and *P* value < 0.05 in all-against-all (more stringent). NABX and ABX enriched families were colored in blue and red, respectively.

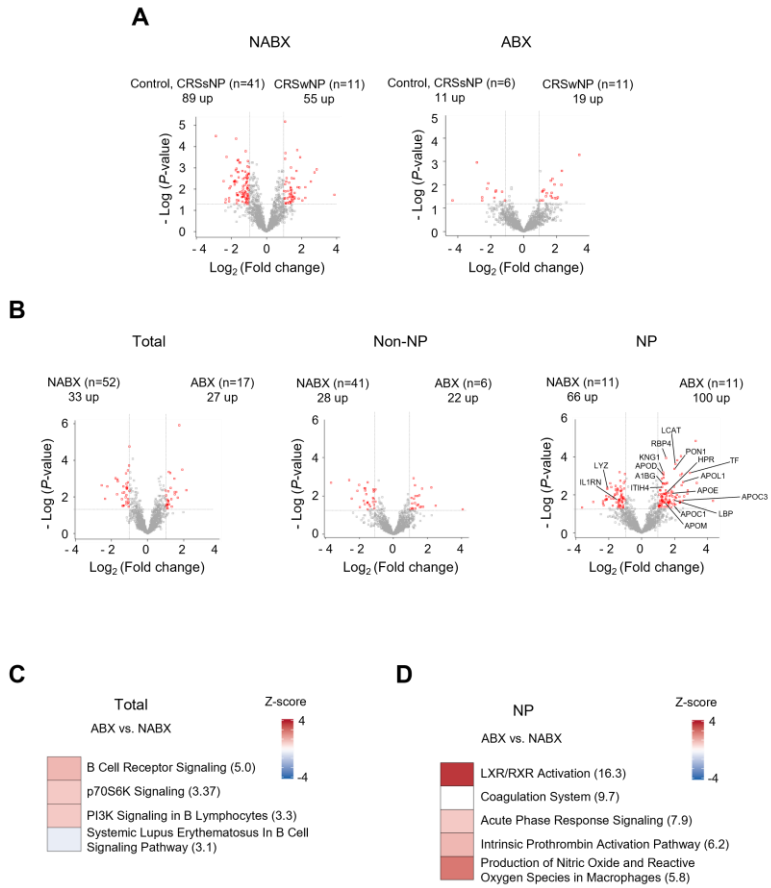

Figure 21. Differences in proteome from nasal secretions in relation to the use of antibiotics

(A, B) Volcano plots showed the $\log_2$ fold change against the negative $\log_{10}$ of *P* value. The horizontal dashed line represented *P* value of 0.05, and the vertical dashed lines represented | $\log_2$ (fold change) | of 1.0. Red squares illustrated proteins with | $\log_2$ (fold change) | ≥ 1.0 and *P* value < 0.05. In the NP subjects, the labeled squares represented proteins involved in LXR/RXR activation. (C, D) Pathway analysis indicating significantly up- or down-regulated pathways in ABX compared to those in NABX group ($P < 0.001$). The pathways were ordered from top to bottom in order of lowest to highest *P* value. The -$\log_{10}$ *P* value were indicated in parenthesis.

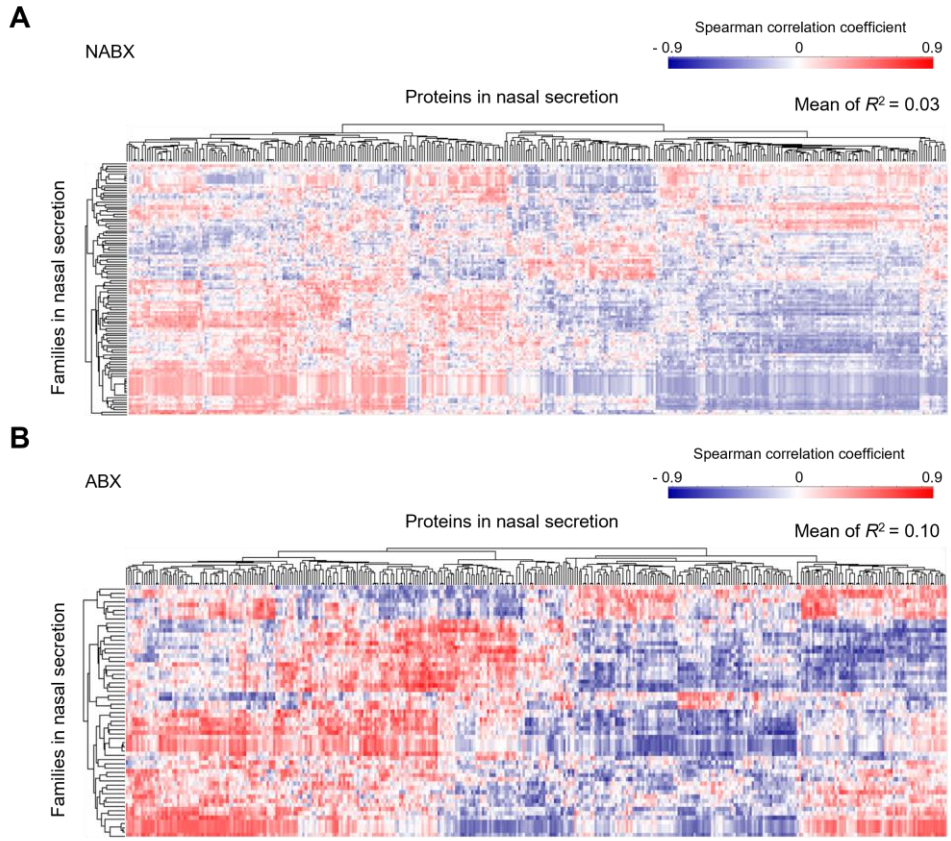

Figure 22. Antibiotic dependent relationships between the microbiome and proteins

Heatmaps showing hierarchical clustering of the top 25 percent families and proteins with high number of significant correlations with each other in the NABX (A) and ABX (B) groups. The means of squared Spearman's correlation coefficients were determined using all the coefficients in the heatmaps.

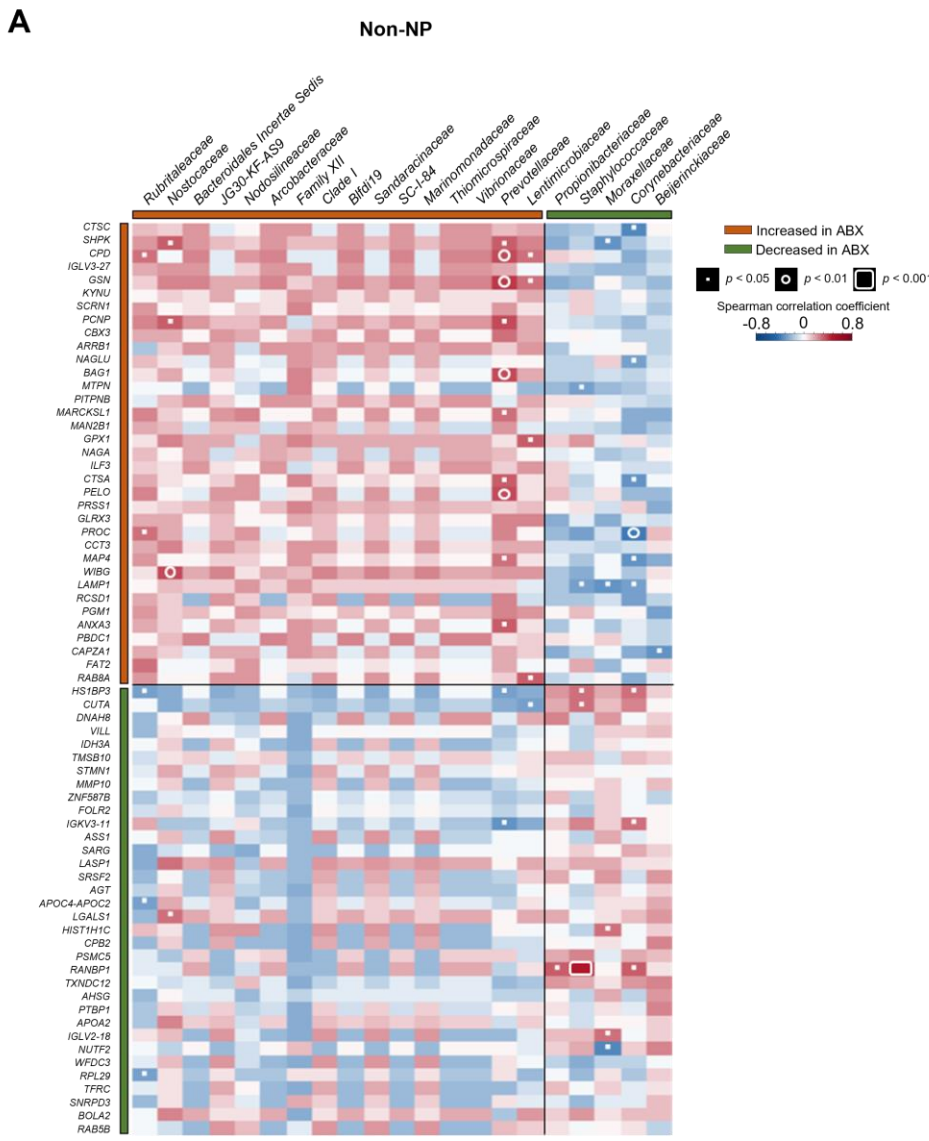
A
Non-NP
Rubritaleaceae
Nostocaceae
Bacteroidales Incertae Sedis
JG30-KF-AS9
Nodosilineaceae
Arcobacteraceae
Family XII
Clade I
Blfdi19
Sandaracinaceae
SC-I-84
Marinomonadaceae
Thiomicrospiraceae
Vibrionaceae
Prevotellaceae
Lentimicrobiaceae
Propionibacteriaceae
Staphylococcaceae
Moraxellaceae
Corynebacteriaceae
Beijerinckiaceae
CTSC
SHPK
CPD
IGLV3-27
GSN
KYNU
SCRN1
PCNP
CBX3
ARRB1
NAGLU
BAG1
MTPN
PITPNB
MARCKSL1
MAN2B1
GPX1
NAGA
ILF3
CTSA
PELO
PRSS1
GLRX3
PROC
CCT3
MAP4
WIBG
LAMP1
RCSD1
PGM1
ANXA3
PBDC1
CAPZA1
FAT2
RAB8A
HS1BP3
CUTA
DNAH8
VILL
IDH3A
TMSB10
STMN1
MMP10
ZNF587B
FOLR2
IGKV3-11
ASS1
SARG
LASP1
SRSF2
AGT
APOC4-APOC2
LGALS1
HIST1H1C
CPB2
PSMC5
RANBP1
TXNDC12
AHSG
PTBP1
APOA2
IGLV2-18
NUTF2
WFDC3
RPL29
TFRC
SNRPD3
BOLA2
RAB5B
Increased in ABX
Decreased in ABX
p < 0.05
p < 0.01
p < 0.001
Spearman correlation coefficient
-0.8
0
0.8

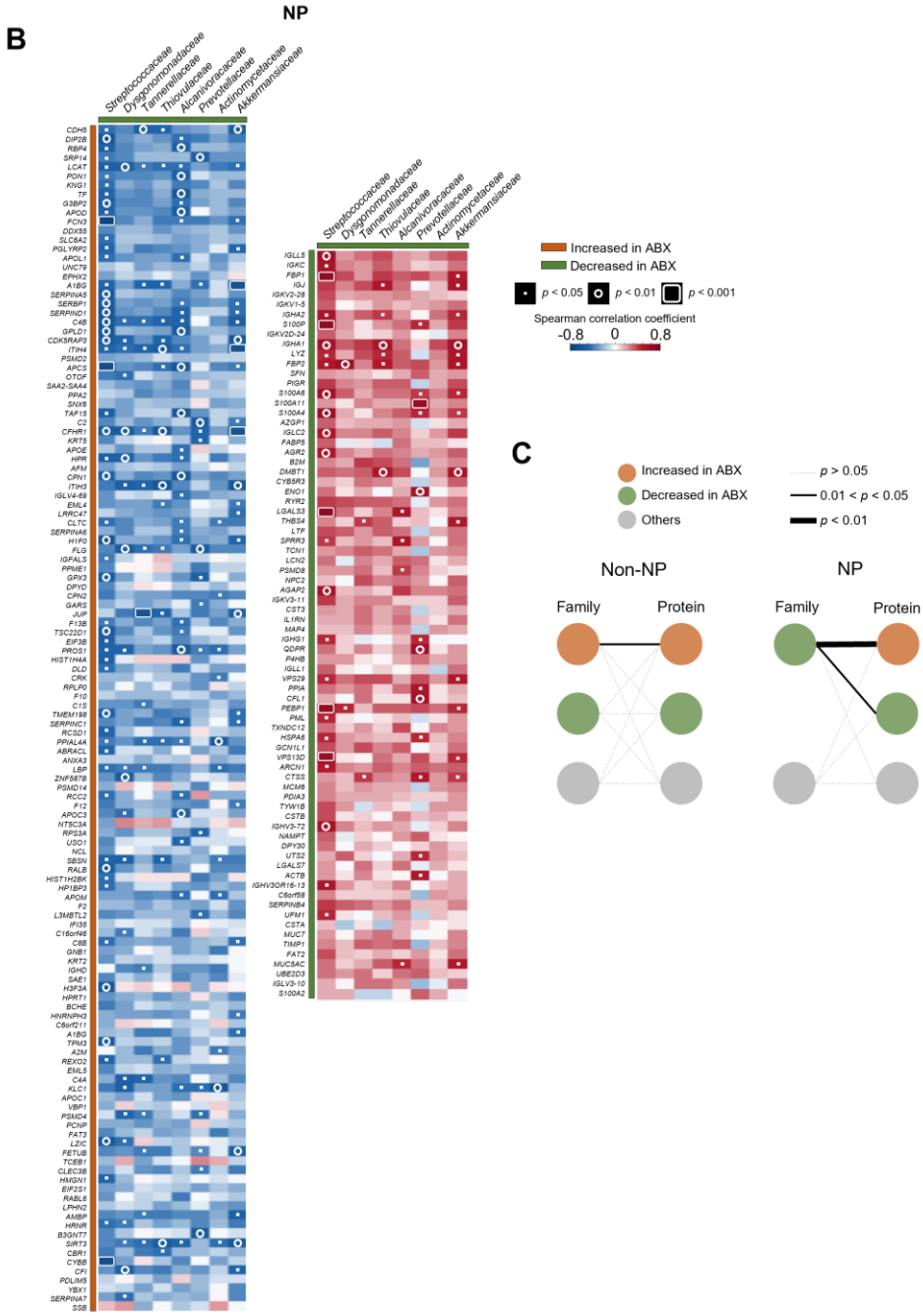
B
NP
Streptococcaceae
Dysgonomonadaceae
Tannerellaceae
Thiovulaceae
Alcanivoraceae
Prevotellaceae
Actinomycetaceae
Akkermansiaceae
Increased in ABX
Decreased in ABX
p < 0.05
p < 0.01
p < 0.001
Spearman correlation coefficient
-0.8
0
0.8
C
Increased in ABX
Decreased in ABX
Others
p > 0.05
0.01 < p < 0.05
p < 0.01
Non-NP
NP
Family
Protein

Figure 23. Antibiotic dependent relationships between up- or down-regulated families and proteins in the ABX group

Heatmaps of the secreted proteins (Student's t-test, $P < 0.05$) and families (Mann-Whitney U test, $P < 0.05$) in the Non-NP (A) and NP (B) subjects. The proteins and families were ordered from top to bottom and from left to right in order of lowest to highest *P* value, respectively. Orange and green colors represented families and proteins significantly enriched in the ABX and NABX, respectively. Redundant microbiome and proteins were ruled out. (C) Associations between families and proteins were significantly enriched in the ABX and NABX groups in the Non-NP and NP subjects, respectively (aSPC, $P < 0.05$). Orange and green colors indicated the same groups previously described in (A, B). Families and proteins were not included in the orange and green colors were considered as Others (colored in gray).

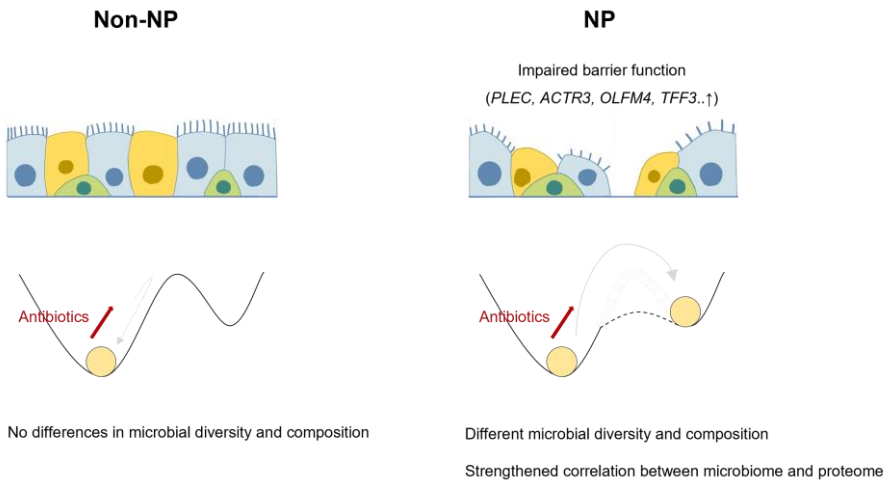

Figure 24. Graphical summary of differential effects of antibiotics in patients with NP

As PLEC, ACTR3, OLFM4, and TFF3 were known to induce epithelial–mesenchymal transition (EMT),[61-64] it could lead to impaired epithelial barrier function. Thus, the perturbations by antibiotics could easily shift the microbiome toward a different equilibrium only in CRSwNP.

Table 3. Method comparison between this study and previous proteomic studies on human nasal sample

Journal	Sample	Sampling method	Target disease
This study	Nasal secretions	filter papers	CRS
Biswas et al.[9]	Nasal mucus	swabs	CRS
Tomazic et al.[57]	Nasal mucus	suction	AR
Mortstedt et al.[56]	Nasal lavage fluid	nasal lavages	Rhinitis
Tomazic et al.[58]	Nasal mucus	suction	AR
Ndika et al.[42]	Nasal epithelium	brushing	AR

CRS, chronic rhinosinusitis; AR, allergic rhinitis

Table 4. Total cell number and the percentage of eosinophils and neutrophils in cohort1①

Sample	Total cell	Eosinophils	Eosinophil (%)	Neutrophils	Neutrophil (%)
CRSsNP_1	551	103	18.69	27	4.9
CRSsNP_2	1640	0	0	0	0
CRSsNP_3	1871	5	0.27	0	0
CRSsNP_4	1026	226	22.03	1	0.1
CRSsNP_5	1805	3	0.17	385	21.33
CRSwNP_1	955	6	0.63	28	2.93
CRSwNP_2	355	0	0	0	0
CRSwNP_3	NA	NA	NA	NA	NA
CRSwNP_4	1345	12	0.89	25	1.86
CRSwNP_5	702	19	2.71	10	1.42

CRS, chronic rhinosinusitis; CRSwNP, chronic rhinosinusitis with nasal polyp

① 보라매병원 김대우 교수님께서 분석해 주셨음.

Table 5. Up- or down-regulated proteins in CRSwNP both in the DDA and DIA set

Cluster	Gene name	Protein name
Up-regulated proteins in CRSwNP		
	BPIFB1	BPI fold-containing family B member 1
	CLTC	Clathrin heavy chain 1
	CRYM	Ketimine reductase mu-crystallin
	FTH1	Ferritin heavy chain
	FTL	Ferritin light chain
	GAA	Lysosomal alpha-glucosidase
	GLUL	Glutamine synthetase
	PFKP	ATP-dependent 6-phosphofructokinase, platelet type
	PGM3	Phosphoacetylglucosamine mutase
	USP5	Ubiquitin carboxyl-terminal hydrolase 5
Down-regulated proteins in CRSwNP		
	CALML5	Calmodulin-like protein 5
	COTL1	Coactosin-like protein
	ERO1L	ERO1-like protein alpha
	FKBP4	Peptidyl-prolyl cis-trans isomerase FKBP4
	HBA2	HCG1745306, isoform CRA_a
	HBD	Hemoglobin subunit delta
	LMNB1	Lamin-B1
	PABPC1	Polyadenylate-binding protein 1
	REXO2	Oligoribonuclease, mitochondrial
	RNASE3	Eosinophil cationic protein
	S100A7	Protein S100-A7
	SERPINB13	Serpin B13
	SERPINB8	Serpin B8
	SRI	Sorcin

Table 6. Differentially expressed proteins with | $\log_2$ (fold change) | ≥ 1.0 and *P* value < 0.05 between control, CRSsNP, and CRSwNP

Accession number		Gene name	Log_2 (Fold change)	- Log (*P* value)
CRSsNP vs. Control	Q9NYQ8	*FAT2*	3.02	1.55
	P04003	*C4BPA*	1.39	2.69
	A6PVU8	*TUFT1*	1.38	1.42
	A0A087X0P6	*IGKV2D-29*	1.37	3.29
	P01031	*C5*	1.35	3.31
	P23142	*FBLN1*	1.33	4.69
	A0A087WSX0	*IGLV5-45*	1.31	1.94
	P02747	*C1QC*	1.29	1.59
	P01616		1.29	2.10
	P08236	*GUSB*	1.13	1.61
	Q6P4A8	*PLBD1*	1.12	1.36
	P01825		1.03	2.03
	A0A087X0N5	*IGKV1-17*	1.02	2.06
	Q96QK1	*VPS35*	1.01	1.37
	P68871	*HBB*	-2.57	2.09
	G3V1N2	*HBA2*	-2.39	1.41
	P02042	*HBD*	-2.30	1.91
	P69905	*HBA1*	-2.28	1.79
	P00915	*CA1*	-2.24	1.68
	P69891	*HBG1*	-2.00	1.74
	O15195	*VILL*	-1.61	1.33
	P62328	*TMSB4X*	-1.11	1.90
	P81605	*DCD*	-1.11	2.33
	P00918	*CA2*	-1.08	2.07
	E9PN89	*HSPA8*	-1.05	1.35
CRSwNP vs. Control	Q9NYQ8	*FAT2*	3.43	1.80
	H3BT29	*PML*	1.98	1.61
	A0A075B6K3	*IGLV2-11*	1.97	2.45
	A0A087WVM2	*CD177*	1.89	2.23
	Q8WXI7	*MUC16*	1.83	3.06
	Q86UN6	*AKAP14*	1.71	2.03
	A0A075B7D0	*IGHV1OR15-1*	1.68	2.01
	Q6UX06	*OLFM4*	1.66	1.67
	P36222	*CHI3L1*	1.51	1.80
	C9JC71	*FCGR3A*	1.49	1.45
	P01773		1.46	3.57
	Q92743	*HTRA1*	1.46	1.70
	P01615		1.45	1.71
	A0A075B6H9	*IGLV4-69*	1.44	1.34
	A0A075B6R9	*IGKV2D-24*	1.43	3.01
	P01708		1.43	2.39
	P59665	*DEFA1*	1.38	2.20
	P13671	*C6*	1.36	1.84
	A0A087X0N5	*IGKV1-17*	1.31	3.22
	O75884	*RBBP9*	1.28	2.06
	A0A087X0P6	*IGKV2D-29*	1.28	2.49
	A0A075B7B8	*IGHV3OR16-12*	1.28	3.86
	Q5T5Y3	*CAMSAP1*	1.26	1.66
	A0A096LPK4	*MUC5AC*	1.25	2.72
	Q15782	*CHI3L2*	1.24	1.50

P15328	*FOLR1*	1.24	1.70
P29401	*TKT*	1.23	2.51
P05089	*ARG1*	1.22	1.62
P01707		1.19	1.67
Q07654	*TFF3*	1.15	1.97
Q9UBG3	*CRNN*	1.14	2.03
P01825		1.14	2.37
O75348	*ATP6V1G1*	1.12	2.18
P49788	*RARRES1*	1.11	1.42
P08236	*GUSB*	1.10	1.55
A0A087X0S5	*COL6A1*	1.08	1.67
P01031	*C5*	1.08	2.18
Q6ZVX7	*NCCRP1*	1.07	1.62
P23142	*FBLN1*	1.06	3.05
Q9BZG9	*LYNX1*	1.06	2.83
P61006	*RAB8A*	1.03	2.52
P04209		1.01	1.46
A0A075B6S3	*IGKV2-30*	1.01	1.63
O14773	*TPP1*	1.01	1.39
B1AKG0	*CFHR1*	1.01	1.53
Q02383	*SEMG2*	1.00	1.46
P04745	*AMY1A*	1.00	2.27
G3V1N2	*HBA2*	-3.30	2.37
P69905	*HBA1*	-2.78	2.51
P69891	*HBG1*	-2.60	2.31
P68871	*HBB*	-2.56	2.38
P00915	*CA1*	-2.54	1.96
P02042	*HBD*	-2.51	2.20
P09210	*GSTA2*	-1.91	1.61
Q6UWW0	*LCN15*	-1.87	1.66
P11684	*SCGB1A1*	-1.79	4.03
O15195	*VILL*	-1.67	2.75
A0A096LPE2	*SAA2-SAA4*	-1.67	1.92
P42331-6	*ARHGAP25*	-1.67	2.65
E9PN89	*HSPA8*	-1.52	2.86
P16050	*ALOX15*	-1.52	1.46
P19338	*NCL*	-1.47	2.42
P62857	*RPS28*	-1.40	2.11
Q96KN2	*CNDP1*	-1.38	1.87
C9J0K6	*SRI*	-1.38	1.74
P40394	*ADH7*	-1.33	2.24
F6WQW2	*RANBP1*	-1.32	2.96
Q96C23	*GALM*	-1.29	2.18
P02647	*APOA1*	-1.25	2.68
J3QL71	*SCRN2*	-1.22	2.05
P00326	*ADH1C*	-1.21	1.52
Q13442	*PDAP1*	-1.19	1.76
Q13228	*SELENBP1*	-1.17	2.04
P02768	*ALB*	-1.16	2.39
P02652	*APOA2*	-1.15	2.05
P00918	*CA2*	-1.13	2.16
A6NGP5	*HN1L*	-1.10	1.66
Q9H477	*RBKS*	-1.09	1.53
Q13885	*TUBB2A*	-1.09	1.53
P02794	*FTH1*	-1.07	1.35
P61956	*SUMO2*	-1.06	2.44
Q9H0E9	*BRD8*	-1.06	1.77
M0R0K9	*TRIM28*	-1.03	1.62
P09382	*LGALS1*	-1.02	3.26
B8ZZQ6	*PTMA*	-1.01	1.51

CRSwNP vs. CRSsNP	C9JZR7	*ACTB*	2.08	1.92
	Q86UN6	*AKAP14*	1.76	2.27
	Q04695	*KRT17*	1.51	2.09
	B4DDF4	*CNN2*	1.45	2.85
	Q9UBG3	*CRNN*	1.45	2.07
	P20930	*FLG*	1.40	1.57
	Q86UX7	*FERMT3*	1.39	2.19
	Q7Z5R6	*APBB1IP*	1.36	1.97
	P05089	*ARG1*	1.28	1.34
	Q8WXI7	*MUC16*	1.27	1.66
	A0A087X188	*BIN2*	1.22	1.78
	Q92743	*HTRA1*	1.21	2.05
	Q9Y376	*CAB39*	1.20	1.48
	Q9NUQ9	*FAM49B*	1.19	2.23
	A0A075B6R9	*IGKV2D-24*	1.19	2.37
	P52790	*HK3*	1.18	1.59
	Q9Y678	*COPG1*	1.17	2.32
	P84085	*ARF5*	1.14	2.63
	Q6UWP8	*SBSN*	1.14	1.89
	P29401	*TKT*	1.11	2.68
	O00203	*AP3B1*	1.08	2.00
	P19878	*NCF2*	1.08	1.59
	Q9Y490	*TLN1*	1.06	2.20
	P26583	*HMGB2*	1.06	2.05
	O75348	*ATP6V1G1*	1.04	2.66
	Q13838	*DDX39B*	1.04	1.41
	P10644	*PRKAR1A*	1.02	1.56
	A0A087WV46	*LAMTOR4*	1.02	1.40
	Q9HC84	*MUC5B*	1.01	1.61
	B1AH77	*RAC2*	1.01	1.49
	P09210	*GSTA2*	-2.28	2.71
	A6PVU8	*TUFT1*	-2.03	3.17
	Q13938	*CAPS*	-2.03	2.26
	Q96C23	*GALM*	-1.64	2.77
	Q13885	*TUBB2A*	-1.55	2.54
	C9J0K6	*SRI*	-1.53	3.24
	P04003	*C4BPA*	-1.49	3.01
	P02747	*C1QC*	-1.44	2.26
	P00326	*ADH1C*	-1.41	3.00
	A0A096LPE2	*SAA2-SAA4*	-1.40	1.59
	P62857	*RPS28*	-1.39	1.62
	P08263	*GSTA1*	-1.37	1.95
	Q9BW30	*TPPP3*	-1.37	1.84
	Q9H477	*RBKS*	-1.36	2.45
	P51857	*AKR1D1*	-1.33	1.59
	P40394	*ADH7*	-1.29	2.28
	P11117	*ACP2*	-1.26	2.41
	P06576	*ATP5B*	-1.25	3.17
	P12277	*CKB*	-1.23	1.78
	P48595	*SERPINB10*	-1.18	1.71
	Q8WVM8	*SCFD1*	-1.11	1.49
	Q01105	*SET*	-1.06	2.27
	Q99733	*NAP1L4*	-1.06	2.24
	K7EIJ8	*KATNAL2*	-1.04	2.19
	P23141	*CES1*	-1.04	1.62
	A6NGP5	*HN1L*	-1.04	1.53
	Q8TD06	*AGR3*	-1.03	1.60
	Q13740	*ALCAM*	-1.02	3.20

Table 7. GO molecular functions of proteins in IPc and DPc group

	GO Term	- Log(adj.*P*-value)
IPc group		
	Cadherin Binding	1.44
DPc group		
	Cholesterol Transfer Activity	2.82
	Sterol Transfer Activity	2.82
	Transition Metal Ion Binding	2.75
	Phosphatidylcholine-Sterol O-acyltransferase Activator Activity	2.75
	Apolipoprotein Receptor Binding	2.75
	Arylesterase Activity	2.75
	Telomeric DNA Binding	2.66
	Heme Binding	2.66
	RNA Binding	2.39
	Copper Ion Binding	2.38
	Endopeptidase Inhibitor Activity	2.38
	Hyaluronic Acid Binding	2.10
	Lipoprotein Particle Receptor Binding	1.56
	Protein Homodimerization Activity	1.46
	Peptidase Inhibitor Activity	1.35

Table 8. Differentially expressed proteins with | log_2 (fold change) | ≥ 1.0 and *P* value < 0.05 between Non-NP and NP in NABX and ABX, respectively

Accession number		Gene name	Log_2 (Fold change)	- Log (*P* value)
Non-NP vs. NP in NABX	Q9NYQ8	*FAT2*	3.87	1.72
	A8MTF8	*FAM3B*	2.86	2.93
	Q9Y230	*RUVBL2*	2.74	2.78
	C9JZR7	*ACTB*	2.52	2.36
	H3BT29	*PML*	2.22	1.59
	A0A087WVM2	*CD177*	2.21	2.08
	P15814	*IGLL1*	2.06	1.46
	A0A075B6R9	*IGKV2D-24*	1.92	3.51
	Q9GZZ8	*LACRT*	1.87	2.07
	Q86UN6	*AKAP14*	1.84	1.55
	P61626	*LYZ*	1.78	2.08
	A0A096LPK4	*MUC5AC*	1.75	3.83
	P47897	*QARS*	1.70	2.86
	P04206		1.61	1.60
	P01778		1.61	1.82
	Q96S96	*PEBP4*	1.59	1.54
	P01708		1.57	2.49
	Q14240-2	*EIF4A2*	1.53	1.64
	Q92882	*OSTF1*	1.51	1.42
	Q6UX06	*OLFM4*	1.50	1.49
	P18065	*IGFBP2*	1.48	1.62
	Q6P5S2	*C6orf58*	1.47	1.69
	A0A075B7D0	*IGHV1OR15-1*	1.44	1.46
	P20827	*EFNA1*	1.43	1.95
	Q9UBC9	*SPRR3*	1.43	2.51
	O75884	*RBBP9*	1.42	1.69
	P15328	*FOLR1*	1.41	1.56
	Q5T5Y3	*CAMSAP1*	1.41	1.83
	Q07654	*TFF3*	1.40	2.04
	Q9HC84	*MUC5B*	1.40	1.78
	P29401	*TKT*	1.39	3.01
	Q9Y678	*COPG1*	1.38	1.97
	A0A087WV46	*LAMTOR4*	1.37	2.09
	Q8WXI7	*MUC16*	1.37	1.35
	A0A087WZB2	*TYW1B*	1.37	1.39
	P49788	*RARRES1*	1.31	1.41
	Q14204	*DYNC1H1*	1.31	1.63
	Q86SQ4	*GPR126*	1.30	1.76
	P00387-3	*CYB5R3*	1.29	2.30
	J3KNB4	*CAMP*	1.29	1.34
	D6REX3	*SEC31A*	1.23	1.91
	P01615		1.21	1.57
	Q9UBG3	*CRNN*	1.19	1.35
	A0A087WXT3	*ZNF33B*	1.15	2.52
	P84085	*ARF5*	1.12	2.36
	Q9BRX2	*PELO*	1.09	1.32
	P80188	*LCN2*	1.09	3.69
	P01833	*PIGR*	1.09	1.89
	P09417	*QDPR*	1.07	1.34

H0YL18	*B2M*	1.06	2.24
A0A075B6S8	*IGKV1-5*	1.06	5.17
A0A087X0N5	*IGKV1-17*	1.06	1.57
P01621		1.05	3.43
P78324	*SIRPA*	1.02	1.55
P01773		1.00	1.90
A0A096LPE2	*SAA2-SAA4*	-2.88	4.51
B0YIW2	*APOC3*	-2.44	2.37
P69905	*HBA1*	-2.35	1.38
P69891	*HBG1*	-2.33	1.51
P42331-6	*ARHGAP25*	-2.27	3.52
E7ETZ0	*CALM1*	-2.14	1.56
P34931	*HSPA1L*	-2.13	1.42
G3V2U4	*UNC79*	-2.11	2.03
K7ER74	*APOC4-APOC2*	-2.06	2.11
P33151	*CDH5*	-2.02	2.61
P22891	*PROZ*	-1.86	2.36
P19338	*NCL*	-1.83	2.21
K7ERI9	*APOC1*	-1.83	2.33
C9J0K6	*SRI*	-1.79	2.38
O75636	*FCN3*	-1.79	2.37
Q96KN2	*CNDP1*	-1.75	2.90
Q99733	*NAP1L4*	-1.73	4.38
P02649	*APOE*	-1.71	2.97
O14791	*APOL1*	-1.70	1.80
P04114	*APOB*	-1.70	1.47
Q6UWW0	*LCN15*	-1.70	1.33
Q9H477	*RBKS*	-1.69	2.33
G3V0E5	*TFRC*	-1.66	1.71
P11684	*SCGB1A1*	-1.65	1.70
Q6P387	*C16orf46*	-1.65	2.81
P27169	*PON1*	-1.65	3.36
P02747	*C1QC*	-1.62	1.71
P62701	*RPS4X*	-1.61	3.38
Q13885	*TUBB2A*	-1.61	2.80
H0Y8X4	*DNPH1*	-1.58	1.46
E9PIA8	*PPT1*	-1.58	2.55
P02652	*APOA2*	-1.55	3.25
P23141	*CES1*	-1.52	1.85
P02647	*APOA1*	-1.49	3.25
P80108	*GPLD1*	-1.41	1.61
P62857	*RPS28*	-1.40	1.78
Q05BV3	*EML5*	-1.39	1.90
Q15056	*EIF4H*	-1.38	2.85
G3XAL9	*SLC12A2*	-1.38	1.64
P16050	*ALOX15*	-1.37	1.40
Q9H4G0-2	*EPB41L1*	-1.34	2.01
P52597	*HNRNPF*	-1.34	2.47
Q96C23	*GALM*	-1.33	2.14
P04180	*LCAT*	-1.32	1.69
A6NNI4	*CD9*	-1.30	1.81
Q9UBE0	*SAE1*	-1.28	1.74
P02794	*FTH1*	-1.27	1.64
Q8WVM8	*SCFD1*	-1.24	1.88
O95445	*APOM*	-1.23	2.19
Q15046	*KARS*	-1.23	2.53
P62805	*HIST1H4A*	-1.23	1.34
D6R967	*PPA2*	-1.21	2.83
P05455	*SSB*	-1.19	3.78
A2A274	*ACO2*	-1.19	1.86

	Q14126	*DSG2*	-1.18	1.55
	P06576	*ATP5B*	-1.15	2.53
	P11117	*ACP2*	-1.15	2.28
	P04003	*C4BPA*	-1.15	1.40
	P01023	*A2M*	-1.14	2.32
	A6NGP5	*HN1L*	-1.14	1.57
	P09622	*DLD*	-1.14	1.50
	Q15257	*PPP2R4*	-1.13	2.64
	P00326	*ADH1C*	-1.12	1.37
	O94760	*DDAH1*	-1.12	1.76
	P98160	*HSPG2*	-1.11	1.68
	Q8WZA0	*LZIC*	-1.10	2.50
	Q9H0E9	*BRD8*	-1.10	2.02
	O00410	*IPO5*	-1.10	1.56
	O43175	*PHGDH*	-1.09	1.30
	P68371	*TUBB4B*	-1.09	2.65
	Q15121	*PEA15*	-1.09	2.37
	Q96NY7	*CLIC6*	-1.09	2.05
	P12277	*CKB*	-1.08	1.54
	P22792	*CPN2*	-1.07	2.11
	B7WNR0	*ALB*	-1.07	3.07
	J3QL71	*SCRN2*	-1.07	1.30
	P00734	*F2*	-1.07	2.72
	D6W5Y5	*CIRBP*	-1.06	1.42
	H3BM11	*SLC6A2*	-1.06	3.32
	P06727	*APOA4*	-1.06	2.53
	Q9H977	*WDR54*	-1.05	1.76
	Q9BX68	*HINT2*	-1.05	1.66
	Q9NQ48	*LZTFL1*	-1.04	1.70
	J3KN67	*TPM3*	-1.02	1.96
	Q9BW04	*SARG*	-1.02	1.53
	Q03154	*ACY1*	-1.01	2.18
	F5GX07	*REXO2*	-1.01	2.73
	P07355	*ANXA2*	-1.01	2.71
	C9JF17	*APOD*	-1.00	3.03
Non-NP vs. NP in ABX	Q86UN6	*AKAP14*	3.39	3.28
	P33151	*CDH5*	2.31	2.60
	Q9UGM5	*FETUB*	2.28	1.99
	P20930	*FLG*	2.08	1.46
	P13671	*C6*	2.00	1.42
	Q6UWP8	*SBSN*	1.89	1.42
	E9PBS1	*PAICS*	1.88	2.01
	A6NLN1	*PTBP1*	1.76	2.26
	P04180	*LCAT*	1.74	1.44
	P62263	*RPS14*	1.71	1.66
	Q9BZG9	*LYNX1*	1.66	2.18
	P00748	*F12*	1.66	1.53
	O43390	*HNRNPR*	1.39	1.63
	P05198	*EIF2S1*	1.36	1.50
	E7ETH6	*ZNF587B*	1.23	1.79
	P02753	*RBP4*	1.15	1.73
	P10643	*C7*	1.15	1.33
	E9PEB5	*FUBP1*	1.13	1.70
	P01019	*AGT*	1.00	1.32
	Q9NYQ8	*FAT2*	-4.34	1.34
	E7EVA0	*MAP4*	-2.86	2.96
	P51857	*AKR1D1*	-2.54	1.45
	A0A087WW55	*PRSS1*	-2.53	1.33
	O76003	*GLRX3*	-2.23	1.84

P48595	*SERPINB10*	-2.16	2.06
O00757	*FBP2*	-1.78	1.44
P52895	*AKR1C2*	-1.72	1.70
Q04828	*AKR1C1*	-1.70	1.75
P17050	*NAGA*	-1.32	1.70
Q9BRP8	*WIBG*	-1.14	1.33

Table 9. Differentially expressed proteins with | log_2 (fold change) | ≥ 1.0 and *P* value < 0.05 between NABX and ABX in total, Non-NP, and NP, respectively

Accession number		Gene name	Log_2 (Fold change)	- Log (*P* value)
NABX vs. ABX in total	A0A075B6H9	*IGLV4-69*	2.14	2.37
	P00742	*F10*	1.91	3.50
	Q9UN86	*G3BP2*	1.76	5.91
	P08779	*KRT16*	1.68	1.95
	P36222	*CHI3L1*	1.59	2.26
	P05160	*F13B*	1.51	2.14
	E7END6	*PROC*	1.51	2.26
	Q7Z5R6	*APBB1IP*	1.49	3.00
	P20930	*FLG*	1.34	1.47
	Q6P4A8	*PLBD1*	1.33	1.87
	P11234	*RALB*	1.29	2.49
	B7ZKW8	*RCSD1*	1.26	3.30
	B4DUR8	*CCT3*	1.20	1.58
	H0YLA2	*SRP14*	1.18	3.36
	B1AKG0	*CFHR1*	1.16	2.30
	P07948-2	*LYN*	1.15	1.79
	Q9Y376	*CAB39*	1.13	1.67
	P80217	*IFI35*	1.13	1.75
	Q8WXI7	*MUC16*	1.11	1.35
	P78371	*CCT2*	1.09	1.48
	P18428	*LBP*	1.09	1.57
	E9PG40	*APP*	1.08	1.85
	P29350	*PTPN6*	1.08	1.59
	C9JB55	*TF*	1.06	1.35
	Q86YZ3	*HRNR*	1.03	2.07
	P27361	*MAPK3*	1.02	1.53
	P13647	*KRT5*	1.01	2.35
	Q5THJ4	*VPS13D*	-2.55	2.63
	O14948	*TFEC*	-2.37	1.89
	O15195	*VILL*	-2.23	2.56
	F6TR53	*HS1BP3*	-1.78	3.01
	P47929	*LGALS7*	-1.70	2.14
	H0YLI6	*IDH3A*	-1.68	2.96
	A0A087WZW8	*IGKV3-11*	-1.65	2.85
	P21964	*COMT*	-1.42	1.87
	P01742		-1.38	2.23
	Q14258	*TRIM25*	-1.38	1.51
	A0A087WZG4	*ARHGEF18*	-1.37	1.50
	P01703		-1.33	2.57
	P01778		-1.32	1.52
	P62328	*TMSB4X*	-1.31	2.25
	P01699		-1.22	1.98
	P63313	*TMSB10*	-1.20	3.29
	P01772		-1.18	2.71
	P40394	*ADH7*	-1.17	2.10
	P62857	*RPS28*	-1.17	1.61
	P01700		-1.17	1.74
	P01763		-1.17	2.51
	F8VXU5	*VPS29*	-1.14	2.44

	F8VVT9	*AGAP2*	-1.14	2.46
	H7BZJ3	*PDIA3*	-1.13	2.55
	P04792	*HSPB1*	-1.10	2.80
	K7EJC1	*PSMD8*	-1.10	1.64
	F6WQW2	*RANBP1*	-1.09	3.44
	Q96C23	*GALM*	-1.09	1.87
	B8ZZQ6	*PTMA*	-1.06	1.70
	P16403	*HIST1H1C*	-1.05	1.46
	P01876	*IGHA1*	-1.02	3.70
	O95881	*TXNDC12*	-1.01	4.76
	P06703	*S100A6*	-1.01	2.32
NABX vs. ABX in Non-NP	Q9NYQ8	*FAT2*	4.06	1.31
	A0A087WW55	*PRSS1*	2.49	1.50
	O75976	*CPD*	2.24	2.45
	E7END6	*PROC*	1.75	1.45
	A0A075B6J3	*IGLV3-27*	1.68	2.39
	B4DUR8	*CCT3*	1.62	1.44
	E7EVA0	*MAP4*	1.56	1.43
	Q16719	*KYNU*	1.52	2.05
	A0A087WUQ6	*GPX1*	1.45	1.54
	P01781		1.42	2.01
	Q9BRX2	*PELO*	1.39	1.51
	P12429	*ANXA3*	1.29	1.33
	Q12765	*SCRN1*	1.29	1.99
	Q9UHJ6	*SHPK*	1.27	2.55
	P48739	*PITPNB*	1.27	1.63
	Q13185	*CBX3*	1.20	1.86
	P53634	*CTSC*	1.19	2.94
	B7ZKW8	*RCSD1*	1.14	1.35
	O00754	*MAN2B1*	1.11	1.61
	P11279	*LAMP1*	1.10	1.35
	Q8WW12	*PCNP*	1.05	1.90
	Q9BVG4	*PBDC1*	1.00	1.33
	O15195	*VILL*	-3.65	2.69
	F6TR53	*HS1BP3*	-2.59	2.82
	K7ER74	*APOC4-APOC2*	-2.45	1.86
	A0A087WZW8	*IGKV3-11*	-2.12	2.26
	H0YLI6	*IDH3A*	-2.01	2.58
	G3V0E5	*TFRC*	-1.96	1.41
	P16403	*HIST1H1C*	-1.73	1.75
	P01772		-1.70	2.41
	P01699		-1.68	1.58
	E7EU04	*FOLR2*	-1.66	2.28
	P63313	*TMSB10*	-1.66	2.41
	Q9BW04	*SARG*	-1.60	2.09
	P01703		-1.54	1.65
	P01700		-1.52	1.31
	A0A075B6F3	*DNAH8*	-1.52	2.72
	P62195	*PSMC5*	-1.52	1.68
	P02652	*APOA2*	-1.43	1.55
	F2Z2G4	*WFDC3*	-1.36	1.45
	P01608		-1.21	1.70
	J3KP15	*SRSF2*	-1.20	1.90
	P16949	*STMN1*	-1.18	2.35
	P00966	*ASS1*	-1.15	2.22
	P09382	*LGALS1*	-1.14	1.83
	A0A075B6J9	*IGLV2-18*	-1.14	1.53
	E7ETH6	*ZNF587B*	-1.12	2.30
	P62318	*SNRPD3*	-1.11	1.37

	A0A087WSY5	*CPB2*	-1.05	1.71
	P09238	*MMP10*	-1.05	2.35
NABX vs. ABX in NP	P01775		4.33	1.68
	G3V2U4	*UNC79*	3.34	2.62
	P33151	*CDH5*	3.27	4.84
	C9JB55	*TF*	2.92	3.15
	A0A096LPE2	*SAA2-SAA4*	2.80	2.24
	A0A075B6H9	*IGLV4-69*	2.78	2.06
	P05160	*F13B*	2.58	1.91
	O14791	*APOL1*	2.52	2.66
	B0YIW2	*APOC3*	2.50	1.68
	Q9UN86	*G3BP2*	2.44	3.11
	P80108	*GPLD1*	2.43	2.51
	Q9P265	*DIP2B*	2.38	4.03
	O75636	*FCN3*	2.36	3.04
	F8WBL1	*L3MBTL2*	2.33	1.60
	A0A087WUS7	*IGHD*	2.32	1.57
	D6RAT0	*RPS3A*	2.31	1.66
	P62805	*HIST1H4A*	2.29	1.89
	H0YLA2	*SRP14*	2.17	3.82
	P20930	*FLG*	2.14	2.00
	P00742	*F10*	2.09	1.83
	P04180	*LCAT*	2.05	3.63
	Q05BV3	*EML5*	2.04	1.49
	P09622	*DLD*	2.03	1.89
	P27169	*PON1*	1.98	3.38
	Q96JB5	*CDK5RAP3*	1.97	2.43
	P18428	*LBP*	1.97	1.72
	P31942	*HNRNPH3*	1.97	1.54
	K7ERI9	*APOC1*	1.94	1.48
	B1AKG0	*CFHR1*	1.89	2.15
	P14923	*JUP*	1.87	1.92
	F8WF14	*BCHE*	1.82	1.55
	Q9Y570	*PPME1*	1.80	1.97
	P04839	*CYBB*	1.79	1.35
	Q9UNH7	*SNX6*	1.79	2.20
	P02649	*APOE*	1.78	2.09
	Q6UWP8-2	*SBSN*	1.73	1.64
	B7ZKW8	*RCSD1*	1.69	1.75
	P11234	*RALB*	1.69	1.63
	P41250	*GARS*	1.68	1.93
	P80217	*IFI35*	1.67	1.60
	Q9UGM5	*FETUB*	1.63	1.44
	Q9UBE0	*SAE1*	1.63	1.56
	Q6P387	*C16orf46*	1.62	1.59
	P13647	*KRT5*	1.62	2.09
	P35908	*KRT2*	1.57	1.58
	P19338	*NCL*	1.56	1.65
	Q8NFL0	*B3GNT7*	1.55	1.38
	P34913	*EPHX2*	1.54	2.62
	P00739	*HPR*	1.53	2.09
	P22792	*CPN2*	1.51	1.93
	P07305	*H1F0*	1.50	2.01
	P05154	*SERPINA5*	1.49	2.60
	P02753	*RBP4*	1.49	3.94
	Q9Y536	*PPIAL4A*	1.48	1.75
	Q9HC10	*OTOF*	1.47	2.24
	C9JXI5	*TMEM198*	1.46	1.79
	P43652	*AFM*	1.46	2.07
	P05388	*RPLP0*	1.46	1.85

Q06033	*ITIH3*	1.44	2.06
O95445	*APOM*	1.42	1.61
P05546	*SERPIND1*	1.42	2.56
Q86YZ3	*HRNR*	1.41	1.38
Q8N1G4	*LRRC47*	1.38	2.04
O60814	*HIST1H2BK*	1.37	1.62
F5H5U2	*DDX55*	1.33	2.89
C9JF17	*APOD*	1.32	3.05
P15169	*CPN1*	1.32	2.06
Q9P1F3	*ABRACL*	1.31	1.74
P01042-2	*KNG1*	1.31	3.18
P04217-2	*A1BG*	1.30	2.60
P07358	*C8B*	1.30	1.59
Q8NC51	*SERBP1*	1.30	2.59
Q5SSJ5	*HP1BP3*	1.30	1.62
P55884	*EIF3B*	1.28	1.90
Q9H0P0-1	*NT5C3A*	1.26	1.68
P00748	*F12*	1.26	1.69
Q14624	*ITIH4*	1.24	2.40
Q9P258	*RCC2*	1.24	1.70
E9PM52	*SIRT3*	1.24	1.37
A0A087X232	*C1S*	1.23	1.80
Q8WW12	*PCNP*	1.22	1.45
P12429	*ANXA3*	1.22	1.73
H3BM11	*SLC6A2*	1.22	2.85
Q12882	*DPYD*	1.21	1.94
B4DEB1	*H3F3A*	1.21	1.56
B5MBZ0	*EML4*	1.20	2.04
P07225	*PROS1*	1.18	1.90
D6R967	*PPA2*	1.14	2.23
J3KN67	*TPM3*	1.13	1.51
Q8WZA0	*LZIC*	1.13	1.45
P00734	*F2*	1.12	1.61
P02743	*APCS*	1.11	2.25
O00487	*PSMD14*	1.11	1.70
Q8TDW7	*FAT3*	1.10	1.45
P05114	*HMGN1*	1.09	1.40
P05198	*EIF2S1*	1.08	1.40
Q96HC4	*PDLIM5*	1.07	1.35
A0A087WVQ6	*CLTC*	1.07	2.02
P55036	*PSMD4*	1.05	1.46
Q3YEC7	*RABL6*	1.03	1.39
Q9NYQ8	*FAT2*	-3.62	1.33
Q5THJ4	*VPS13D*	-2.95	1.62
H3BT29	*PML*	-2.35	1.67
A0A087WZB2	*TYW1B*	-2.35	1.54
P47929	*LGALS7*	-2.31	1.45
P15814	*IGLL1*	-2.22	1.72
A0A087WZW8	*IGKV3-11*	-2.18	1.76
P01778		-2.15	1.94
E7EVA0	*MAP4*	-2.14	1.73
P01742		-2.10	1.79
P61626	*LYZ*	-2.10	2.38
P01833	*PIGR*	-2.08	2.32
P02788	*LTF*	-1.99	1.89
P01877	*IGHA2*	-1.91	2.60
P01876	*IGHA1*	-1.86	2.41
P01703		-1.85	1.79
Q6P5S2	*C6orf58*	-1.75	1.42
K7EJC1	*PSMD8*	-1.69	1.80

Q9UBC9	*SPRR3*	-1.69	1.88
Q9UGM3	*DMBT1*	-1.62	2.02
P00387-3	*CYB5R3*	-1.62	2.00
P06703	*S100A6*	-1.59	2.28
P25815	*S100P*	-1.57	2.47
Q14566	*MCM6*	-1.54	1.60
Q01469	*FABP5*	-1.49	2.15
H0YL18	*B2M*	-1.49	2.04
O00757	*FBP2*	-1.48	2.34
P25311	*AZGP1*	-1.47	2.26
P48594	*SERPINB4*	-1.44	1.39
P31949	*S100A11*	-1.43	2.27
F8VXU5	*VPS29*	-1.41	1.72
P01772		-1.40	1.56
Q8TAX7	*MUC7*	-1.39	1.35
Q9C005	*DPY30*	-1.38	1.49
Q92616	*GCN1L1*	-1.38	1.62
P18510-2	*IL1RN*	-1.37	1.74
F8VVT9	*AGAP2*	-1.34	1.77
A0A087WYR4	*IGLL5*	-1.34	3.19
P01708		-1.32	1.45
A0A075B7E8	*IGHV3OR16-13*	-1.30	1.43
P01621		-1.30	2.19
P01591	*IGJ*	-1.29	2.75
P23528	*CFL1*	-1.28	1.69
A0A075B6R9	*IGKV2D-24*	-1.27	2.42
A0A075B6K4	*IGLV3-10*	-1.27	1.31
P17931	*LGALS3*	-1.25	1.92
P20061	*TCN1*	-1.25	1.85
P06733	*ENO1*	-1.24	1.96
A0A075B6K9	*IGLC2*	-1.23	2.22
O95994	*AGR2*	-1.22	2.06
P26447	*S100A4*	-1.21	2.27
H7BZJ3	*PDIA3*	-1.20	1.59
P01034	*CST3*	-1.20	1.75
P17066	*HSPA6*	-1.16	1.64
E7ES19	*THBS4*	-1.16	1.90
P61960	*UFM1*	-1.15	1.36
A0A096LPK4	*MUC5AC*	-1.14	1.33
P60709	*ACTB*	-1.13	1.44
P80188	*LCN2*	-1.12	1.80
P04207		-1.11	1.85
A0A075B6S8	*IGKV1-5*	-1.09	2.62
P01610		-1.07	1.81
P31947	*SFN*	-1.05	2.32
A0A087WYL9	*IGKC*	-1.03	3.10
A0A087X1V9	*IGKV2-28*	-1.02	2.73
A0A087WV47	*IGHG1*	-1.01	1.73

DISCUSSION

To my knowledge, this is the first report on the effects of antibiotics on the microbiome, secreted proteome, and associations between them in CRS using multi-omics. Expectedly, the use of antibiotics could diminish differences in the microbial community and secreted proteome in relation to disease status. Interestingly, I revealed the use of antibiotics might have stronger effects on not only nasal microbiome and secreted proteome, but also associations between them in CRSwNP compared to those in control and CRSsNP subjects. On the other hand, proteomic analysis of the nasal secretions on the filter papers identified approximately three times higher number of proteins than previous studies. The possible reason could be explained by that the filter papers provided a solid protein-stabilizing matrix blocking the cytokine-mediated protein neutralization and protein degradation.[12, 13]

I speculated that the differential effects of antibiotics in CRSwNP could be caused by impaired barrier function of epithelial cells. The down-regulation of tight junction proteins like occludin-1 and Zo-1 and defective epithelial barrier by IL-4 are common features in CRSwNP.[65-67] In this study, proteins, which were significantly increased across control, CRSsNP, and CRSwNP subjects, were associated with cadherin binding (Table 7). The term contains *USO1*, *SEPTIN2*, *SEPTIN7*, *OLFM4*, and *PLEC*. *USO1* is critical for mitotic spindle and plays an important role in apoptosis.[68] Septins are essential to polarization of epithelial cells.[69] *OLFM4* and *PLEC* promote epithelial–mesenchymal transition (EMT) process.[61, 63] In addition, *ACTR3* and *TFF3*, which were significantly up-regulated across control, CRSsNP, and CRSwNP, are known to induce EMT. [62, 64] On the

other hand, a previous study has suggested a simple quantitative model based on a stability landscape conception.[70] According to the report, the microbiome are in multiple stable equilibria of landscape, however, sufficiently strong perturbations like antibiotics could alter the microbiome from its normal equilibrium to other states. Because of the impaired epithelial barrier function in CRSwNP, I speculated the perturbations by antibiotics could easily shift the microbiome toward a different equilibrium only in CRSwNP. Furthermore, the perturbations could have stronger effects on associations between microbiome and proteome (Fig. 24).

It remains controversial as to whether the alpha diversity is increased or decreased in CRS patients compared to control.[6, 9, 19-21, 23-26, 28, 30-32, 71] Generally, these studies excluded patients who had taken antibiotics within approximately one month prior to sampling, although antibiotics are prescribed frequently to patients with CRS.[17, 18] A study had demonstrated gut microbial richness was significantly decreased over approximately 6 months following antibiotic perturbation.[72] Therefore, differences in alpha diversity between control and CRS subjects should be analyzed by considering the use of antibiotics. In present study, Shannon and Simpson indices were significantly increased across control, CRSsNP and CRSwNP subjects (Fig. 10A). I believe that it is the results from real-world cohorts.

I sought to identify up- or down-regulated proteins in CRSwNP both in the DDA and DIA set. Interestingly, *FTL* and *FTH1* were significantly upregulated in CRSwNP (Fig. 8B) and are known as components of ferritin.[73] As ferritin level in serum is a well-known marker of inflammation, it is increased in patients with various inflammatory conditions such as autoimmune diseases.[74] However, the association between nasal polyps and iron metabolism is unknown and further studies are required.

Most of families that were increased in control were aerobes, while most of families that were increased in CRSwNP were anaerobes (Fig. 13A). *Propionibacteriaceae* and *Caulobacteraceae*, which were significantly decreased in CRSwNP, are known as the most common families in healthy nasal mucosa.[75, 76] *Ruminococcaceae* is significantly decreased in Crohn's disease patients[77] and it was dominant in control. *Prevotellaceae* was significantly increased across control, CRSsNP, and CRSwNP. The deficiency of NLRP6 inflammasome in murine colonic epithelial cell results in exacerbation of colitis and increase of *Prevotellaceae*.[78]

The IPA analysis revealed that the most significantly increased terms was LXR/RXR activation term in the ABX compared to the NABX group in NP subjects (Fig. 21D). Several studies have reported that Liver X receptor (LXR) activation exerted anti-inflammatory functions by acting as a strong suppressor of pro-inflammatory processes.[79-81] In addition, it can induce regulatory T cells.[82] On the other hand, a partial retinoid X receptors (RXR) agonist, CBt-PMN, reduces the production of pro-inflammatory cytokines like *Tnf* and *Il6* in DSS-induced colitis model.[83] Also, in a murine model of emphysema, treatment with NEt-4IB, another partial RXR agonist, significantly induces the anti-oxidant activity and suppresses the progression of airway remodeling by inhibiting expression of VEGF.[84] Moreover, in Fig. 23B, *Actinomycetaceae* significantly decreased in the ABX compared to NABX. It is known as dominant family in nasal lavage of asthma patients.[85] In addition, *S100A11* and *MUC5AC*, which were significantly decreased in the ABX group, are known to be up-regulated in CRSwNP.[86, 87] *S100A4* could promote EMT process in CRS [88] and its expression is significantly down-regulated

in the ABX group. Based on these reports, I speculated that antibiotics might have beneficial effects to treat CRSwNP.

On the other hand, antibiotics might negatively affect the treatment of CRSwNP. In Fig. 23B, *Streptococcaceae* was significantly decreased in the ABX compared to NABX while its relative abundance is increased in healthy control compared to allergic rhinitis patients.[89] In addition, *KNG1*, which was significantly up-regulated in the ABX group, shows increased expression in mucus from CRSwNP compared to control.[90] *PIGR* and *AZGP1* are known to be significantly decreased in CRSwNP compared to control[91, 92] and their expression was significantly down-regulated in the ABX group. These results help to understand how antibiotics, which are used to relieve symptoms of CRS, affect the treatment of CRS.

There were some limitations in present study. As antibiotics are prescribed frequently to patients with CRS, a relatively small number of subjects who taken antibiotics was included in control than in CRSsNP and CRSwNP. Thus, further studies with similar proportions of subjects who had taken antibiotics are needed. Moreover, to verify the association between nasal microbiome and host responses in relation to the use of antibiotics, a larger sample size will be required.

In conclusion, I identify large number of proteins from nasal secretions on the filter papers compared to previous studies. Using the sampling technique, I reveal the associations between the microbiome and secreted proteome could be altered in relation to the use of antibiotics. In addition, the correlation between them is strengthened in subjects who had taken antibiotics. Especially, antibiotics could have different effects on the association in the non-NP and NP group. I identify the use of antibiotics might have stronger effects on not only nasal microbiome and secreted proteome, but also associations between them in CRSwNP compared to

those in control and CRSsNP subjects. However, it is not clear whether the global changes caused by antibiotics are favorable or unfavorable to treat CRS. I suggest that the use of antibiotics need to be regarded as an essential confounding factor in the microbiome and proteome analysis, especially in CRSwNP patients. These findings allow us to obtain new insight on the nasal environment and host response in CRS.

REFERENCES

1. Fokkens, WJ; Lund, VJ; Mullol, J; Bachert, C; Alobid, I; Baroody, F, et al., EPOS 2012: European position paper on rhinosinusitis and nasal polyps 2012. A summary for otorhinolaryngologists. Rhinology 2012;50:1-12.

2. Hirsch, AG; Stewart, WF; Sundaresan, AS; Young, AJ; Kennedy, TL; Scott Greene, J, et al., Nasal and sinus symptoms and chronic rhinosinusitis in a population-based sample. Allergy 2017;72:274-281.

3. Zhang, Y; Gevaert, E; Lou, H; Wang, X; Zhang, L; Bachert, C, et al., Chronic rhinosinusitis in Asia. J Allergy Clin Immunol 2017;140:1230-1239.

4. Tomassen, P; Vandeplas, G; Van Zele, T; Cardell, LO; Arebro, J; Olze, H, et al., Inflammatory endotypes of chronic rhinosinusitis based on cluster analysis of biomarkers. J Allergy Clin Immunol 2016;137:1449-1456 e4.

5. Divekar, R; Patel, N; Jin, J; Hagan, J; Rank, M; Lal, D, et al., Symptom-Based Clustering in Chronic Rhinosinusitis Relates to History of Aspirin Sensitivity and Postsurgical Outcomes. J Allergy Clin Immunol Pract 2015;3:934-40 e3.

6. Cope, EK; Goldberg, AN; Pletcher, SD; Lynch, SV, Compositionally and functionally distinct sinus microbiota in chronic rhinosinusitis patients have immunological and clinically divergent consequences. Microbiome 2017;5:53.

7. Liao, B; Liu, JX; Li, ZY; Zhen, Z; Cao, PP; Yao, Y, et al., Multidimensional endotypes of chronic rhinosinusitis and their association with treatment outcomes. Allergy 2018;73:1459-1469.

8. Klingler, AI; Stevens, WW; Tan, BK; Peters, AT; Poposki, JA; Grammer, LC, et al., Mechanisms and biomarkers of inflammatory endotypes in chronic rhinosinusitis without nasal polyps. Journal of Allergy and Clinical Immunology 2021;147:1306-1317.

9. Biswas, K; Wagner Mackenzie, B; Waldvogel-Thurlow, S; Middleditch, M; Jullig, M; Zoing, M, et al., Differentially Regulated Host Proteins Associated with Chronic Rhinosinusitis Are Correlated with the Sinonasal Microbiome. Front Cell Infect Microbiol

2017;7:504.

10. Wang, BF; Cao, PP; Norton, JE; Poposki, JA; Klingler, AI; Suh, LA, et al., Evidence that oncostatin M synergizes with IL-4 signaling to induce TSLP expression in chronic rhinosinusitis with nasal polyps. J Allergy Clin Immunol 2023.

11. Csosz, E; Kallo, G; Markus, B; Deak, E; Csutak, A; Tozser, J, Quantitative body fluid proteomics in medicine - A focus on minimal invasiveness. J Proteomics 2017;153:30-43.

12. Alam, R; Sim, TC; Hilsmeier, K; Grant, JA, Development of a new technique for recovery of cytokines from inflammatory sites in situ. J Immunol Methods 1992;155:25-9.

13. Badorrek, P; Muller, M; Koch, W; Hohlfeld, JM; Krug, N, Specificity and reproducibility of nasal biomarkers in patients with allergic rhinitis after allergen challenge chamber exposure. Ann Allergy Asthma Immunol 2017;118:290-297.

14. Kreitmaier, P; Katsoula, G; Zeggini, E, Insights from multi-omics integration in complex disease primary tissues. Trends Genet 2023;39:46-58.

15. Lee, JWJ; Plichta, D; Hogstrom, L; Borren, NZ; Lau, H; Gregory, SM, et al., Multi-omics reveal microbial determinants impacting responses to biologic therapies in inflammatory bowel disease. Cell Host Microbe 2021;29:1294-1304 e4.

16. Yan, Z; Chen, B; Yang, Y; Yi, X; Wei, M; Ecklu-Mensah, G, et al., Multi-omics analyses of airway host-microbe interactions in chronic obstructive pulmonary disease identify potential therapeutic interventions. Nat Microbiol 2022;7:1361-1375.

17. Barshak, MB; Durand, ML, The role of infection and antibiotics in chronic rhinosinusitis. Laryngoscope Investig Otolaryngol 2017;2:36-42.

18. Smith, SS; Evans, CT; Tan, BK; Chandra, RK; Smith, SB; Kern, RC, National burden of antibiotic use for adult rhinosinusitis. J Allergy Clin Immunol 2013;132:1230-2.

19. Gan, WG; Yang, FJ; Tang, YP; Zhou, DM; Qing, D; Hu, JJ, et al., The difference in nasal bacterial microbiome diversity between chronic rhinosinusitis patients with polyps and a control population. International Forum of Allergy & Rhinology 2019;9:582-592.

20. Rom, D; Bassiouni, A; Eykman, E; Liu, ZX; Paramasivan, S; Alvarado, R, et al., The Association Between Disease Severity and Microbiome in Chronic Rhinosinusitis. Laryngoscope 2019;129:1265-1273.

21. Mahdavinia, M; Engen, PA; LoSavio, PS; Naqib, A; Khan, RJ; Tobin, MC, et al., The nasal microbiome in patients with chronic rhinosinusitis: Analyzing the effects of atopy and bacterial functional pathways in 111 patients. Journal of Allergy and Clinical Immunology 2018;142:287-290.

22. Biswas, K; Cavubati, R; Gunaratna, S; Hoggard, M; Waldvogel-Thurlow, S; Hong, J, et al., Comparison of Subtyping Approaches and the Underlying Drivers of Microbial Signatures for Chronic Rhinosinusitis. Msphere 2019;4.

23. Paramasivan, S; Bassiouni, A; Shiffer, A; Dillon, MR; Cope, EK; Cooksley, C, et al., The international sinonasal microbiome study: A multicentre, multinational characterization of sinonasal bacterial ecology. Allergy 2020;75:2037-2049.

24. Copeland, E; Leonard, K; Carney, R; Kong, J; Forer, M; Naidoo, Y, et al., Chronic Rhinosinusitis: Potential Role of Microbial Dysbiosis and Recommendations for Sampling Sites. Frontiers in Cellular and Infection Microbiology 2018;8.

25. Chalermwatanachai, T; Vilchez-Vargas, R; Holtappels, G; Lacoere, T; Jauregui, R; Kerckhof, FM, et al., Chronic rhinosinusitis with nasal polyps is characterized by dysbacteriosis of the nasal microbiota. Scientific Reports 2018;8.

26. Lal, D; Keim, P; Delisle, J; Barker, B; Rank, MA; Chia, N, et al., Mapping and comparing bacterial microbiota in the sinonasal cavity of healthy, allergic rhinitis, and chronic rhinosinusitis subjects. Int Forum Allergy Rhinol 2017;7:561-569.

27. Jain, R; Hoggard, M; Biswas, K; Zoing, M; Jiang, YN; Douglas, R, Changes in the bacterial microbiome of patients with chronic rhinosinusitis after endoscopic sinus surgery. International Forum of Allergy & Rhinology 2017;7:7-15.

28. Hoggard, M; Biswas, K; Zoing, M; Mackenzie, BW; Taylor, MW; Douglas, RG, Evidence of microbiota dysbiosis in chronic rhinosinusitis. International Forum of Allergy

& Rhinology 2017;7:230-239.

29. Ramakrishnan, VR; Gitomer, S; Kofonow, JM; Robertson, CE; Frank, DN, Investigation of sinonasal microbiome spatial organization in chronic rhinosinusitis. Int Forum Allergy Rhinol 2017;7:16-23.

30. Biswas, K; Hoggard, M; Jain, R; Taylor, MW; Douglas, RG, The nasal microbiota in health and disease: variation within and between subjects. Frontiers in Microbiology 2015;6.

31. Choi, EB; Hong, SW; Kim, DK; Jeon, SG; Kim, KR; Cho, SH, et al., Decreased diversity of nasal microbiota and their secreted extracellular vesicles in patients with chronic rhinosinusitis based on a metagenomic analysis. Allergy 2014;69:517-526.

32. Aurora, R; Chatterjee, D; Hentzleman, J; Prasad, G; Sindwani, R; Sanford, T, Contrasting the Microbiomes From Healthy Volunteers and Patients With Chronic Rhinosinusitis. Jama Otolaryngology-Head & Neck Surgery 2013;139:1328-1338.

33. Ramakrishnan, VR; Hauser, LJ; Feazel, LM; Ir, D; Robertson, CE; Frank, DN, Sinus microbiota varies among chronic rhinosinusitis phenotypes and predicts surgical outcome. Journal of Allergy and Clinical Immunology 2015;136:334-+.

34. Kim, YS; Han, D; Kim, J; Kim, DW; Kim, YM; Mo, JH, et al., In-Depth, Proteomic Analysis of Nasal Secretions from Patients With Chronic Rhinosinusitis and Nasal Polyps. Allergy Asthma Immunol Res 2019;11:691-708.

35. Kim, YS; Han, D; Mo, JH; Kim, YM; Kim, DW; Choi, HG, et al., Antibiotic-Dependent Relationships Between the Nasal Microbiome and Secreted Proteome Nasal Polyps. Allergy Asthma & Immunology Research 2021;13:589-608.

36. Wisniewski, JR; Gaugaz, FZ, Fast and sensitive total protein and Peptide assays for proteomic analysis. Anal Chem 2015;87:4110-6.

37. Han, D; Jin, J; Woo, J; Min, H; Kim, Y, Proteomic analysis of mouse astrocytes and their secretome by a combination of FASP and StageTip-based, high pH, reversed-phase fractionation. Proteomics 2014;14:1604-1609.

38. Woo, J; Han, D; Park, J; Kim, SJ; Kim, Y, In-depth characterization of the secretome of mouse CNS cell lines by LC-MS/MS without prefractionation. Proteomics 2015;15:3617-22.

39. Lee, H; Kim, K; Woo, J; Park, J; Kim, H; Lee, KE, et al., Quantitative Proteomic Analysis Identifies AHNAK (Neuroblast Differentiation-associated Protein AHNAK) as a Novel Candidate Biomarker for Bladder Urothelial Carcinoma Diagnosis by Liquid-based Cytology. Molecular & Cellular Proteomics 2018;17:1788-1802.

40. Bruderer, R; Bernhardt, OM; Gandhi, T; Miladinovic, SM; Cheng, LY; Messner, S, et al., Extending the limits of quantitative proteome profiling with data-independent acquisition and application to acetaminophen-treated three-dimensional liver microtissues. Mol Cell Proteomics 2015;14:1400-10.

41. Cox, J; Neuhauser, N; Michalski, A; Scheltema, RA; Olsen, JV; Mann, M, Andromeda: a peptide search engine integrated into the MaxQuant environment. J Proteome Res 2011;10:1794-805.

42. Ndika, J; Airaksinen, L; Suojalehto, H; Karisola, P; Fyhrquist, N; Puustinen, A, et al., Epithelial proteome profiling suggests the essential role of interferon-inducible proteins in patients with allergic rhinitis. J Allergy Clin Immunol 2017;140:1288-1298.

43. Cox, J; Hein, MY; Luber, CA; Paron, I; Nagaraj, N; Mann, M, Accurate proteome-wide label-free quantification by delayed normalization and maximal peptide ratio extraction, termed MaxLFQ. Mol Cell Proteomics 2014;13:2513-26.

44. Reiter, L; Rinner, O; Picotti, P; Huttenhain, R; Beck, M; Brusniak, MY, et al., mProphet: automated data processing and statistical validation for large-scale SRM experiments. Nature Methods 2011;8:430-U85.

45. Perez-Riverol, Y; Csordas, A; Bai, J; Bernal-Llinares, M; Hewapathirana, S; Kundu, DJ, et al., The PRIDE database and related tools and resources in 2019: improving support for quantification data. Nucleic Acids Res 2019;47:D442-D450.

46. Tyanova, S; Temu, T; Sinitcyn, P; Carlson, A; Hein, MY; Geiger, T, et al., The

Perseus computational platform for comprehensive analysis of (prote)omics data. Nat Methods 2016;13:731-40.

47. Deeb, SJ; Tyanova, S; Hummel, M; Schmidt-Supprian, M; Cox, J; Mann, M, Machine Learning-based Classification of Diffuse Large B-cell Lymphoma Patients by Their Protein Expression Profiles. Mol Cell Proteomics 2015;14:2947-60.

48. Kuleshov, MV; Jones, MR; Rouillard, AD; Fernandez, NF; Duan, Q; Wang, Z, et al., Enrichr: a comprehensive gene set enrichment analysis web server 2016 update. Nucleic Acids Res 2016;44:W90-7.

49. Caporaso, JG; Kuczynski, J; Stombaugh, J; Bittinger, K; Bushman, FD; Costello, EK, et al., QIIME allows analysis of high-throughput community sequencing data. Nat Methods 2010;7:335-6.

50. Segata, N; Izard, J; Waldron, L; Gevers, D; Miropolsky, L; Garrett, WS, et al., Metagenomic biomarker discovery and explanation. Genome Biol 2011;12:R60.

51. Xu, ZY; Xu, GJ; Pan, W; Neuroimaging, AD, Adaptive testing for association between two random vectors in moderate to high dimensions. Genetic Epidemiology 2017;41:599-609.

52. Kim, MS; Pinto, SM; Getnet, D; Nirujogi, RS; Manda, SS; Chaerkady, R, et al., A draft map of the human proteome. Nature 2014;509:575-81.

53. Hu, A; Noble, WS; Wolf-Yadlin, A, Technical advances in proteomics: new developments in data-independent acquisition. F1000Res 2016;5.

54. Doerr, A, DIA mass spectrometry. Nature Methods 2015;12:35-35.

55. Guo, J; Huan, T, Comparison of Full-Scan, Data-Dependent, and Data-Independent Acquisition Modes in Liquid Chromatography-Mass Spectrometry Based Untargeted Metabolomics. Analytical Chemistry 2020;92:8072-8080.

56. Mortstedt, H; Ali, N; Karedal, M; Jacobsson, H; Rietz, E; Diab, KK, et al., Targeted proteomic analyses of nasal lavage fluid in persulfate-challenged hairdressers with bleaching powder-associated rhinitis. J Proteome Res 2015;14:860-73.

57. Tomazic, PV; Birner-Gruenberger, R; Leitner, A; Spoerk, S; Lang-Loidolt, D, Seasonal proteome changes of nasal mucus reflect perennial inflammatory response and reduced defence mechanisms and plasticity in allergic rhinitis. J Proteomics 2016;133:153-160.

58. Tomazic, PV; Birner-Gruenberger, R; Leitner, A; Obrist, B; Spoerk, S; Lang-Loidolt, D, Nasal mucus proteomic changes reflect altered immune responses and epithelial permeability in patients with allergic rhinitis. J Allergy Clin Immunol 2014;133:741-50.

59. Kumpitsch, C; Koskinen, K; Schopf, V; Moissl-Eichinger, C, The microbiome of the upper respiratory tract in health and disease. BMC Biol 2019;17:87.

60. Kim, MR; Hong, SW; Choi, EB; Lee, WH; Kim, YS; Jeon, SG, et al., Staphylococcus aureus-derived extracellular vesicles induce neutrophilic pulmonary inflammation via both Th1 and Th17 cell responses. Allergy 2012;67:1271-81.

61. Xu, R; He, S; Ma, D; Liang, R; Luo, Q; Song, G, Plectin Downregulation Inhibits Migration and Suppresses Epithelial Mesenchymal Transformation of Hepatocellular Carcinoma Cells via ERK1/2 Signaling. Int J Mol Sci 2022;24.

62. Hu, H; Zhang, S; Xiong, S; Hu, B; He, Y; Gu, Y, ACTR3 promotes cell migration and invasion by inducing epithelial mesenchymal transition in pancreatic ductal adenocarcinoma. J Gastrointest Oncol 2021;12:2325-2333.

63. Gao, XZ; Wang, GN; Zhao, WG; Han, J; Diao, CY; Wang, XH, et al., Blocking OLFM4/HIF-1alpha axis alleviates hypoxia-induced invasion, epithelial-mesenchymal transition, and chemotherapy resistance in non-small-cell lung cancer. J Cell Physiol 2019;234:15035-15043.

64. Yusufu, A; Shayimu, P; Tuerdi, R; Fang, C; Wang, F; Wang, H, TFF3 and TFF1 expression levels are elevated in colorectal cancer and promote the malignant behavior of colon cancer by activating the EMT process. Int J Oncol 2019;55:789-804.

65. Wise, SK; Laury, AM; Katz, EH; Den Beste, KA; Parkos, CA; Nusrat, A, Interleukin-4 and interleukin-13 compromise the sinonasal epithelial barrier and perturb

intercellular junction protein expression. Int Forum Allergy Rhinol 2014;4:361-70.

66. Soyka, MB; Wawrzyniak, P; Eiwegger, T; Holzmann, D; Treis, A; Wanke, K, et al., Defective epithelial barrier in chronic rhinosinusitis: the regulation of tight junctions by IFN-gamma and IL-4. J Allergy Clin Immunol 2012;130:1087-1096 e10.

67. Khalmuratova, R; Park, JW; Shin, HW, Immune Cell Responses and Mucosal Barrier Disruptions in Chronic Rhinosinusitis. Immune Netw 2017;17:60-67.

68. Radulescu, AE; Mukherjee, S; Shields, D, The Golgi protein p115 associates with gamma-tubulin and plays a role in Golgi structure and mitosis progression. J Biol Chem 2011;286:21915-26.

69. Wang, X; Wang, W; Wang, X; Wang, M; Zhu, L; Garba, F, et al., The septin complex links the catenin complex to the actin cytoskeleton for establishing epithelial cell polarity. J Mol Cell Biol 2021;13:395-408.

70. Shaw, LP; Bassam, H; Barnes, CP; Walker, AS; Klein, N; Balloux, F, Modelling microbiome recovery after antibiotics using a stability landscape framework. ISME J 2019;13:1845-1856.

71. Koeller, K; Herlemann, DPR; Schuldt, T; Ovari, A; Guder, E; Podbielski, A, et al., Microbiome and Culture Based Analysis of Chronic Rhinosinusitis Compared to Healthy Sinus Mucosa. Front Microbiol 2018;9:643.

72. Palleja, A; Mikkelsen, KH; Forslund, SK; Kashani, A; Allin, KH; Nielsen, T, et al., Recovery of gut microbiota of healthy adults following antibiotic exposure. Nat Microbiol 2018;3:1255-1265.

73. Arosio, P; Ingrassia, R; Cavadini, P, Ferritins: a family of molecules for iron storage, antioxidation and more. Biochim Biophys Acta 2009;1790:589-99.

74. Zandman-Goddard, G; Shoenfeld, Y, Ferritin in autoimmune diseases. Autoimmun Rev 2007;6:457-63.

75. Bassis, CM; Tang, AL; Young, VB; Pynnonen, MA, The nasal cavity microbiota of healthy adults. Microbiome 2014;2.

76. Zhang, X; Dong, K; Kang, Z; Ji, X; Ning, X; Ma, Q, et al., Characteristics and associations of microbial community in the eye, anterior nares, and oropharynx of healthy adults: eye-nose microbiota transmission. Am J Transl Res 2023;15:2241-2255.

77. Morgan, XC; Tickle, TL; Sokol, H; Gevers, D; Devaney, KL; Ward, DV, et al., Dysfunction of the intestinal microbiome in inflammatory bowel disease and treatment. Genome Biol 2012;13:R79.

78. Elinav, E; Strowig, T; Kau, AL; Henao-Mejia, J; Thaiss, CA; Booth, CJ, et al., NLRP6 inflammasome regulates colonic microbial ecology and risk for colitis. Cell 2011;145:745-57.

79. Jakobsson, T; Vedin, LL; Hassan, T; Venteclef, N; Greco, D; D'Amato, M, et al., The oxysterol receptor LXRbeta protects against DSS- and TNBS-induced colitis in mice. Mucosal Immunol 2014;7:1416-28.

80. Thomas, DG; Doran, AC; Fotakis, P; Westerterp, M; Antonson, P; Jiang, H, et al., LXR Suppresses Inflammatory Gene Expression and Neutrophil Migration through cis-Repression and Cholesterol Efflux. Cell Reports 2018;25:3774-+.

81. Higham, A; Lea, S; Plumb, J; Maschera, B; Simpson, K; Ray, D, et al., The role of the liver X receptor in chronic obstructive pulmonary disease. Respir Res 2013;14:106.

82. Herold, M; Breuer, J; Hucke, S; Knolle, P; Schwab, N; Wiendl, H, et al., Liver X receptor activation promotes differentiation of regulatory T cells. PLoS One 2017;12:e0184985.

83. Onuki, M; Watanabe, M; Ishihara, N; Suzuki, K; Takizawa, K; Hirota, M, et al., A partial agonist for retinoid X receptor mitigates experimental colitis. Int Immunol 2019;31:251-262.

84. Morichika, D; Miyahara, N; Fujii, U; Taniguchi, A; Oda, N; Senoo, S, et al., A retinoid X receptor partial agonist attenuates pulmonary emphysema and airway inflammation. Respir Res 2019;20:2.

85. Chen, MP; He, SY; Miles, P; Li, CL; Ge, YJ; Yu, XC, et al., Nasal Bacterial

Microbiome Differs Between Healthy Controls and Those With Asthma and Allergic Rhinitis. Frontiers in Cellular and Infection Microbiology 2022;12.

86. Liu, C; Du, H; Wang, Y; Gong, N; Qi, W; Zhou, X, et al., S100A11 regulates nasal epithelial cell remodeling and inflammation in CRSwNPs via the RAGE-mediated AMPK-STAT3 pathway. Mol Immunol 2021;140:35-46.

87. Zhang, Y; Derycke, L; Holtappels, G; Wang, XD; Zhang, L; Bachert, C, et al., Th2 cytokines orchestrate the secretion of MUC5AC and MUC5B in IL-5-positive chronic rhinosinusitis with nasal polyps. Allergy 2019;74:131-140.

88. Gong, N; Shi, L; Bing, X; Li, H; Hu, H; Zhang, P, et al., S100A4/TCF Complex Transcription Regulation Drives Epithelial-Mesenchymal Transition in Chronic Sinusitis Through Wnt/GSK-3beta/beta-Catenin Signaling. Front Immunol 2022;13:835888.

89. Chiang, TY; Yang, YR; Zhuo, MY; Yang, F; Zhang, YF; Fu, CH, et al., Microbiome profiling of nasal extracellular vesicles in patients with allergic rhinitis. World Allergy Organ J 2022;15:100674.

90. Kao, SS; Bassiouni, A; Ramezanpour, M; Finnie, J; Chegeni, N; Colella, AD, et al., Proteomic analysis of nasal mucus samples of healthy patients and patients with chronic rhinosinusitis. J Allergy Clin Immunol 2021;147:168-178.

91. Hulse, KE; Norton, JE; Suh, L; Zhong, Q; Mahdavinia, M; Simon, P, et al., Chronic rhinosinusitis with nasal polyps is characterized by B-cell inflammation and EBV-induced protein 2 expression. Journal of Allergy and Clinical Immunology 2013;131:1075-+.

92. Wang, M; Tang, S; Yang, X; Xie, X; Luo, Y; He, S, et al., Identification of key genes and pathways in chronic rhinosinusitis with nasal polyps and asthma comorbidity using bioinformatics approaches. Front Immunol 2022;13:941547.

국문 초록

만성 비부비동염(CRS)은 비강 내에 12주 이상 지속되는 염증질환으로 동서양을 막론하고 가장 빈번히 발생하는 상기도 질환이다. 이 질환은 이질성이 높아, 연구자들은 cytokine, 증상과 미생물의 구성 등의 여러 측면에서 endotype을 밝히고자 하였다.

endotype을 연구하기 위한 비강 샘플은 대부분 biopsy, lavages, swabs, scraping 등의 방법으로 얻었다. 하지만 lavages, swabs와 같이 비침습적 방법으로 얻은 비강 샘플에서는 소변이나 타액 등 다른 비침습적 방식으로 얻은 샘플들에 비해 적은 수의 단백질만을 얻을 수 있었다. 그래서 이 논문에서는 단백질이 쉽게 흡착되고 보존될 수 있는 filter papers를 이용하여 비침습적 방법으로 상대적으로 많은 수의 비강 단백질을 얻고자 하였다.

항생제가 CRS의 증상을 완화시키는데 효과가 있는지는 논란의 여지가 있지만 환자들에게 빈번히 처방이 되고 있다. 하지만 기존의 대부분의 CRS 연구에서는 환자의 항생제 복용 이력은 고려되지 않았다. 그렇기 때문에 현재까지 항생제가 비강 내 미생물과 상피세포에 어떠한 영향을 미치는지 밝혀진 바가 없다.

본 연구는 29명의 질환이 없는 대조군, 30명의 폴립을 동반하지 않은 만성 비부비동염 환자 (CRSsNP) 그리고 40명의 폴립을 동반한 만성 비부비동염 환자 (CRSwNP)를 대상으로 진행되었다. 이 연구를 통해 비강

내 미생물과 분비된 단백질의 연관성이 질환의 상태에 따라 달라질 수 있음을 확인하였다. 더 나아가서 항생제 복용 여부에 따라 미생물과 분비된 단백질의 연관성도 달라짐을 확인하였다. 흥미롭게도 항생제 복용 여부의 영향은 NP (nasal polyps; CRSwNP) 환자와 Non-NP (대조군과 CRSsNP) 그룹에서 다르게 나타났다. Non-NP 그룹에 비해, 항생제는 NP 그룹의 미생물과 분비된 단백질 그리고 그 둘의 상관관계에 더 크게 작용했다. 여전히 항생제가 CRS의 증상 완화에 도움이 되는지는 명확히 알지 못하지만 앞으로 CRS에서의 미생물과 단백질 연구에서 항생제 복용 여부를 중요한 교란 변수로 여겨야 함을 보여주었다. 따라서 본 연구는 CRS에서 비강 내 환경과 host의 반응의 연관성을 통해 질환의 이해를 높이고자 하였으며 항생제가 미생물과 host에 미치는 영향에 대한 새로운 관점을 제시하였다.

주요어: 비부비동염, 비용종, 단백체학, 군유전체학, 항생제

학번: *2017-26948*